Co-funded by the
Erasmus+ Programme
of the European Union

SEAS 4.0

SUSTAINABLE SHIP AND SHIPPING 4.0

Erasmus Mundus Joint Master Degree

www.master-seas40.unina.it

Development of a Thruster-Assisted Single-Point Anchoring Model

Dmitrii Aparin

4 March 2025

Supervisor: Prof. Smilko Rudan

University of Zagreb

Università degli studi di Napoli Federico II

Universidade da Coruna

Academic Year 2024/2025

TUHH
Technische Universität Hamburg

Content overview

Context

- Autonomous small Catamaran project.
- Survey mission for a prolonged periods.
- Anchoring at safe areas for a recharge.
- Risk of anchor dragging.

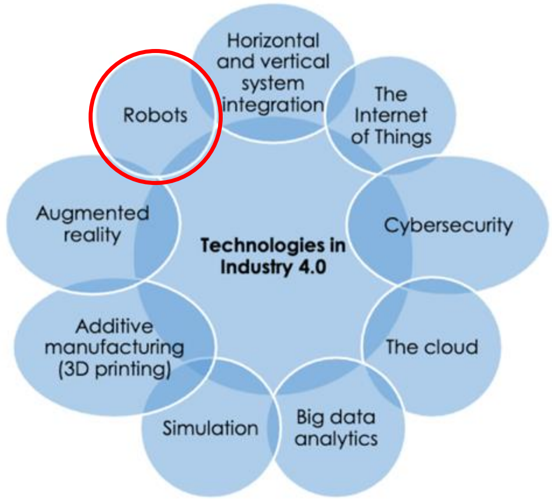

Bahrin et al. 2016

The Otter Uncrewed Surface Vessel. Maritime Robotics

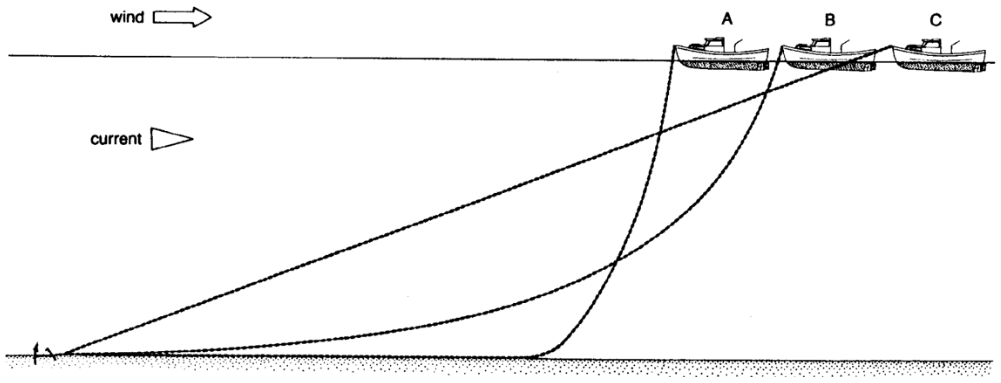

Hinz 1986

Introduction. Anchoring

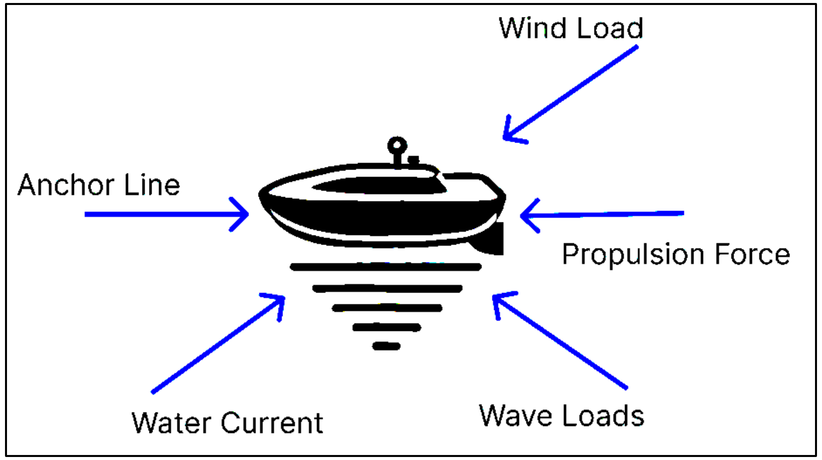

fig. External forces acting on the vessel.

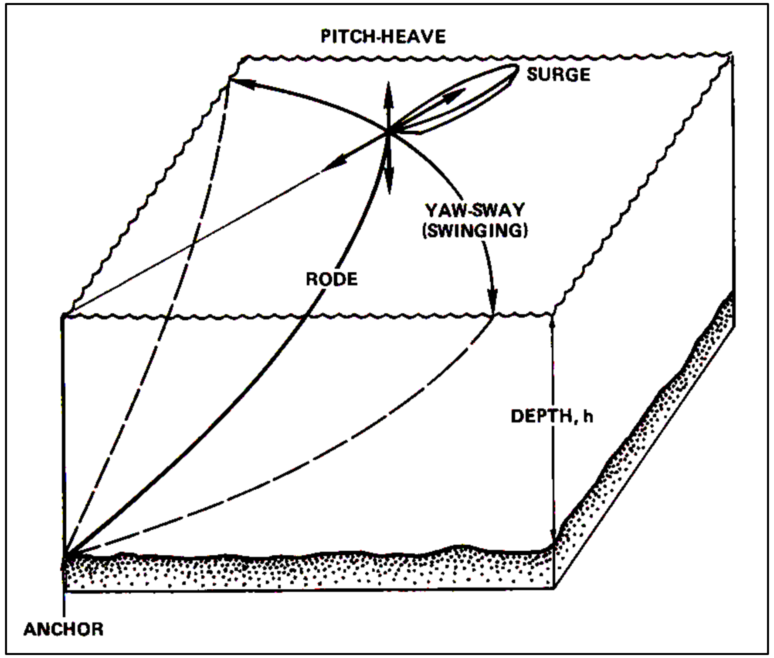

fig. Motions at Anchor.

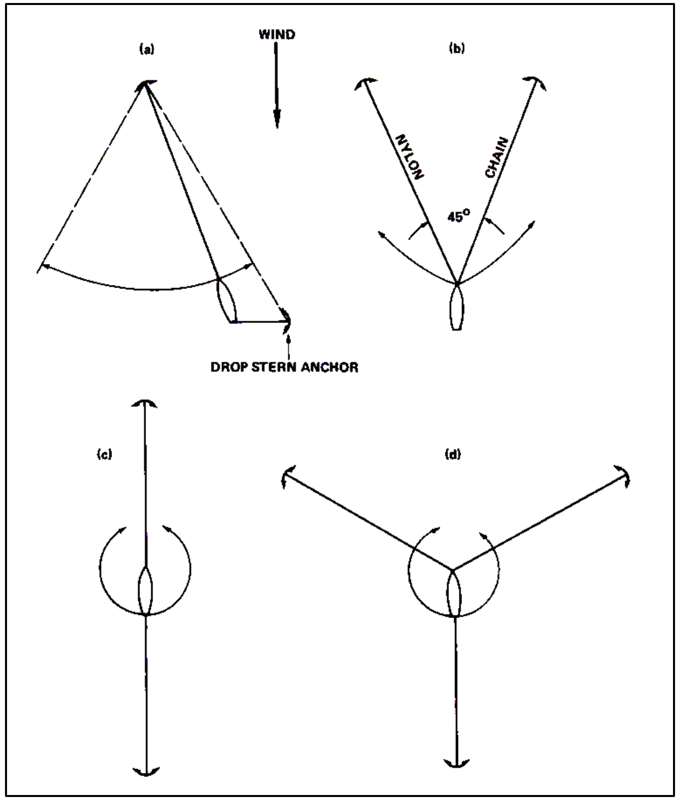

fig. Anchor methods of swinging prevention

Van Dorn 2009

Introduction. Motions at Anchor

Figure 8-1 Some Types of Behavior of Ships at Single Point Moorings

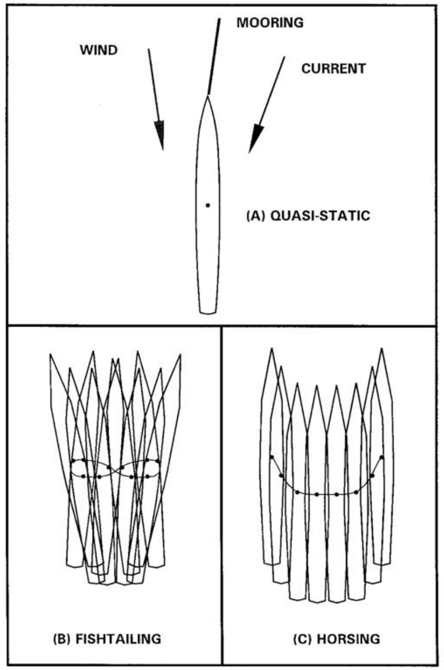

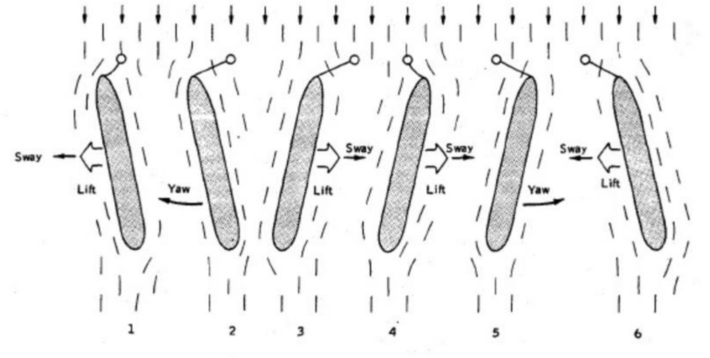

FIG. 3 - MOTION OF VESSEL DUE TO WIND OR CURRENT AT SPM.

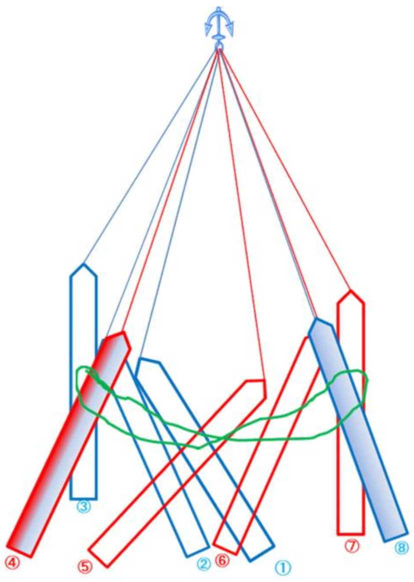

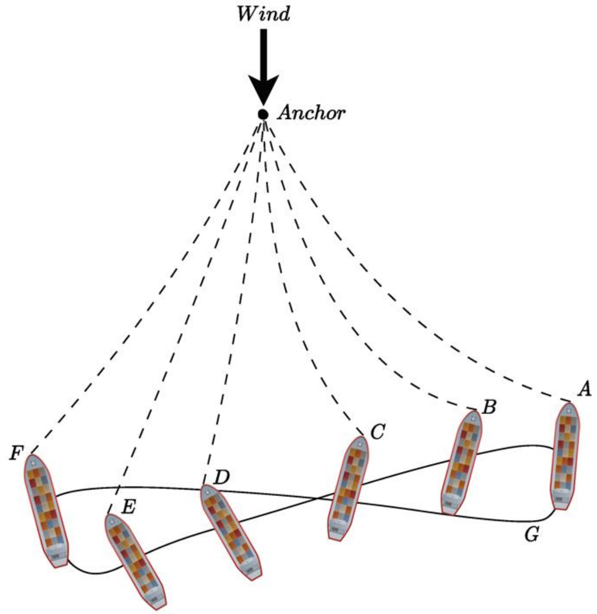

References:

1) US Army Corps of Engineers 2020 (UFC 4-159-03)

2) Flory and Poranski 1977

3) Okada T 2018

4) Yoo et al. 2024

Introduction. Note for small vessels

- **Low Displacement and Inertia:** Small boats have less mass, making them more susceptible to external forces.
- **Vertical Motions:** Heave, pitch, and roll can be pronounced in small vessels due to wave action.
- **Limited Storage and Gear Weight:** Smaller boats require lighter anchors and shorter anchor lines.
- **Reduced Catenary Effect:** A lighter, shorter line means less weight to form a pronounced catenary, increasing the risk of anchor dragging.

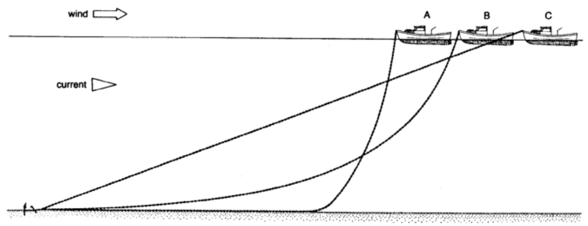

Introduction. Scope

Goal –minimize Tension in the Anchor Line.

Solution – propose a control strategy to actively assist anchoring.

Hypothesis – swinging increases anchor load.

Task – develop a simulator to gain insights to motions of an anchored vessel, with possibility to test control strategies.

- **Initial assumptions:**
  - 3 DoF (only horizontal movements)
  - Anchor is fixed and not dragged
  - Catenary not considered

Development of the model

$$Equations\ of\ motion, 3DoF, expressed\ in\ body-fixed\ frame$$

Core - Fossen's matrix notation:

$$\boxed{\underbrace{\boldsymbol{M}_{RB}\dot{\boldsymbol{\nu}} + \boldsymbol{C}_{RB}(\boldsymbol{\nu})\boldsymbol{\nu}}_{\text{rigid body terms}} + \underbrace{\boldsymbol{M}_A\dot{\boldsymbol{\nu}}_r + \boldsymbol{C}_A(\boldsymbol{\nu}_r)\boldsymbol{\nu}_r + \boldsymbol{D}(\boldsymbol{\nu}_r)\boldsymbol{\nu}_r}_{\text{hydrodynamic terms}} = \boldsymbol{\tau}_{ext}}$$

$$\boldsymbol{M} = \boldsymbol{M}_{RB} + \boldsymbol{M}_A = \begin{bmatrix} m - X_{\dot{u}} & 0 & 0 \\ 0 & m - Y_{\dot{v}} & mx_g - Y_{\dot{r}} \\ 0 & mx_g - N_{\dot{v}} & I_z - N_{\dot{r}} \end{bmatrix},$$

*rigid body
*added mass

$$\boldsymbol{C}_{RB}(\nu) = \begin{bmatrix} 0 & 0 & -m(x_g r + v) \\ 0 & 0 & mu \\ m(x_g r + v) & -mu & 0 \end{bmatrix}, \quad \boldsymbol{C}_A(\nu_r) = \begin{bmatrix} 0 & 0 & c_{13} \\ 0 & 0 & c_{23} \\ -c_{13} & -c_{23} & 0 \end{bmatrix},$$

$$c_{13} = Y_{\dot{v}} v_r + 0.5(N_{\dot{v}} + Y_{\dot{r}})r$$

$$\boldsymbol{D} = \boldsymbol{D}_L + \boldsymbol{D}_{NL}, \qquad c_{23} = -X_{\dot{u}} u_r$$

$$\boldsymbol{D}_L = -\begin{bmatrix} X_u & 0 & 0 \\ 0 & Y_v & Y_r \\ 0 & N_v & N_r \end{bmatrix}, \qquad \boldsymbol{D}_{NL} = -\begin{bmatrix} X_{|u|u}|u_r| & 0 & 0 \\ 0 & Y_{|v|v}|v_r| + Y_{|r|v}|r| & Y_{|v|r}|v_r| + Y_{|r|r}|r| \\ 0 & N_{|v|v}|v_r| + N_{|r|v} r & N_{|v|r}|v| + N_{|r|r}|r| \end{bmatrix}.$$

MMG:

$$\left.\begin{aligned} m(\dot{u} - vr - x_G r^2) &= X_M = X_A + X_S \\ m(\dot{v} + x_G \dot{r} + ur) &= Y_M = Y_A + Y_S \\ I_{zz}\dot{r} + mx_G(\dot{v} + ur) &= N_M = N_{GA} + N_{GS} \end{aligned}\right\}$$

$$\left.\begin{aligned} X_A &= f_{AX}(\dot{u}) = X_{\dot{u}}\dot{u} \\ Y_A &= f_{AY}(\dot{v}, \dot{r}) = Y_{\dot{v}}\dot{v} + Y_{\dot{r}}\dot{r} \\ N_A &= f_{AN}(\dot{v}, \dot{r}) = N_{\dot{v}}\dot{v} + N_{\dot{r}}\dot{r} \\ \\ X_S &= f_{SX}(u, v, r, \delta, n) \\ Y_S &= f_{SY}(u, v, r, \delta, n) \\ N_S &= f_{SN}(u, v, r, \delta, n) \end{aligned}\right\}$$

(Yoshimura 2005)

Development of the model

$$\boldsymbol{x} = [\boldsymbol{\eta} \quad \boldsymbol{\nu}]^T$$

$$\boldsymbol{\eta} = \begin{bmatrix} x \\ y \\ \psi \end{bmatrix}, \qquad \boldsymbol{\nu} = \begin{bmatrix} u \\ v \\ r \end{bmatrix},$$

$$\mathcal{J}(\psi) = \begin{bmatrix} \cos\psi & -\sin\psi & 0 \\ \sin\psi & \cos\psi & 0 \\ 0 & 0 & 1 \end{bmatrix}$$

$$\dot{\boldsymbol{\eta}} = \begin{bmatrix} \dot{x} \\ \dot{y} \\ \dot{\psi} \end{bmatrix} = \mathcal{J}(\psi)\,\boldsymbol{\nu} = \mathcal{J}(\psi) \begin{bmatrix} u \\ v \\ r \end{bmatrix},$$

$$\dot{\boldsymbol{\nu}} = \begin{bmatrix} \dot{u} \\ \dot{v} \\ \dot{r} \end{bmatrix} = \boldsymbol{M}^{-1}(\boldsymbol{\tau}_{ext} - \boldsymbol{C}_{RB}(\boldsymbol{\nu})\boldsymbol{\nu} - \boldsymbol{C}_A(\boldsymbol{\nu}_r)\boldsymbol{\nu}_r - \boldsymbol{D}_{lin}(\boldsymbol{\nu}_r)\boldsymbol{\nu}_r)),$$

$$\boxed{\dot{\boldsymbol{x}} = \boldsymbol{f}(t, \boldsymbol{x}) = \begin{bmatrix} \dot{\boldsymbol{\eta}} \\ \dot{\boldsymbol{\nu}} \end{bmatrix}}$$

Integrate this with numerical method

Euler: $\boldsymbol{x}_{n+1} = \boldsymbol{x}_n + f(t_n, \boldsymbol{x}_n)$

or

Runge-Kutta 4th order: $\boldsymbol{x}_{n+1} = \boldsymbol{x}_n + \frac{\Delta t}{6}(k_1 + 2k_2 + 2k_3 + k_4)$

$$k_1 = f(t_n, \boldsymbol{x}_n)$$

$$k_2 = f\left(t_n + \frac{\Delta t}{2}, \boldsymbol{x}_n + \frac{\Delta t}{2} k_1\right)$$

$$k_3 = f\left(t_n + \frac{\Delta t}{2}, \boldsymbol{x}_n + \frac{\Delta t}{2} k_2\right)$$

$$k_4 = f(t_n + \Delta t, \boldsymbol{x}_n + \Delta t \cdot k_3)$$

**In general RK4 is more accurate*

Development of the model. Wind

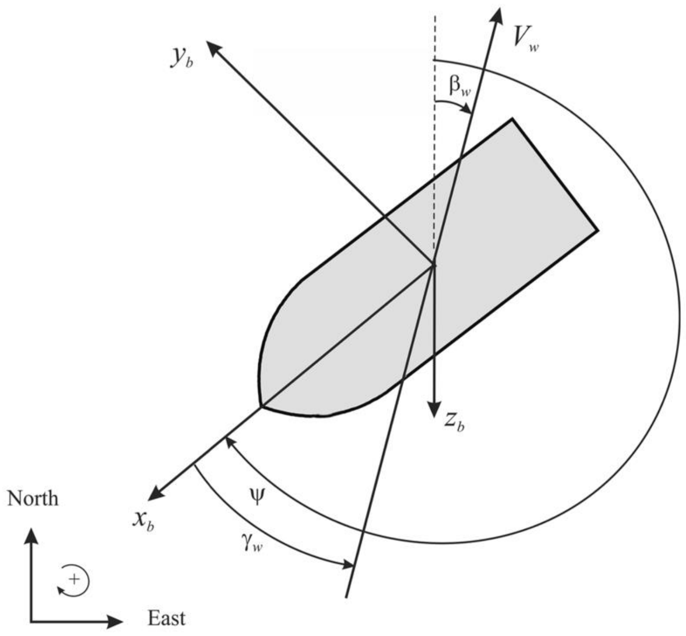

from Fossen (2011)

Wind is assumed to be stationary with a given speed U_{wind} and direction β_{wind} (measured from the global x-axis).
The relative wind velocities in the body frame are:

$$u_{rel} = u - U_{wind}\, cos(\beta_{wind} - \psi)\,, \qquad v_{rel} = v - U_{wind}\, sin(\beta_{wind} - \psi)\,,$$

and the effective wind speed is:

$$U_{rel} = \sqrt{u_{rel}^2 + v_{rel}^2}\,.$$

An aerodynamic drag law is then used to calculate wind forces in body-frame:

$$\tau_{wind,surge} = 0.5\rho_{air}U_{rel}^2\, C_{d,surge}(\gamma)A_{fr}\,,$$

$$\tau_{wind,sway} = 0.5\rho_{air}U_{rel}^2\, C_{d,sway}(\gamma)A_{lat}\,,$$

$$\tau_{wind,yaw} = 0.5\rho_{air}U_{wind,rel}^2\, C_{d,yaw}(\gamma)A_{lat}L_{pp}\,,$$

$$C_{d,surge}(\gamma) = -C_x cos(\gamma)$$
$$C_{d,sway}(\gamma) = C_y sin(\gamma)$$
$$C_{d,yaw}(\gamma) = C_n sin(2\gamma)$$

assumed values:
$C_x = C_y = 5C_N = 0.2$ – racing car profile

Development of the model. Current

The current velocity is initially defined in the global coordinate system, with its speed U_c and direction β.

First, the current velocity components in the global frame are computed as:

$$U_{cx}^{g} = U_c \cos\beta, \qquad U_{cy}^{g} = U_c \sin\beta.$$

In body frame accordingly:

$$\begin{bmatrix} u_c^b \\ v_c^b \end{bmatrix} = \begin{bmatrix} \cos\psi & \sin\psi \\ -\sin\psi & \cos\psi \end{bmatrix} \begin{bmatrix} U_{cx}^{g} \\ U_{cy}^{g} \end{bmatrix} = \begin{bmatrix} U_{cx}^{g}\cos\psi + U_{cy}^{g}\sin\psi \\ -U_{cx}^{g}\sin\psi + U_{cy}^{g}\cos\psi \end{bmatrix}.$$

Vessel's relative velocity with respect to the surrounding water is calculated as:

$$\boldsymbol{\nu_r} = \boldsymbol{\nu} - \boldsymbol{\nu_c^b}, \qquad \boldsymbol{\nu_c^b} = [u_c^b, v_c^b, 0]$$

These relative velocities are then used in:

- The Coriolis force calculations $\boldsymbol{C}_A(\boldsymbol{\nu}_r)$ related to added mass.
- The damping matrix $\boldsymbol{D}(\boldsymbol{\nu}_r)$, since hydrodynamic resistance depends on relative velocity.

Development of the model. Anchor

- External forces ANCHOR

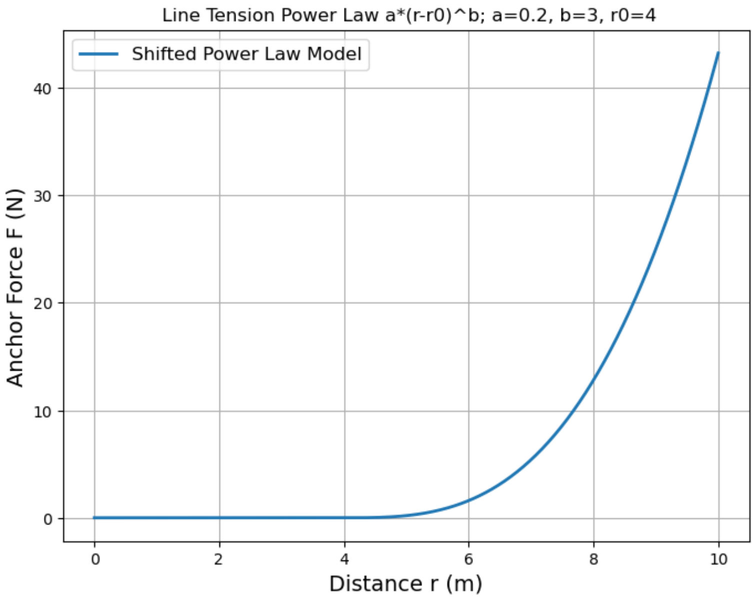

The force magnitude is expressed by the power-law:

$$F_{anchor}(r) = p(r - r_0)^q,$$

where r is the distance from the ship's bow to the anchor point.
r could be found by first determining the bow's position in global frame:

$$x_{bow} = x + \frac{L_{pp}}{2} \cos\psi, \qquad y_{bow} = y + \frac{L_{pp}}{2} \sin\psi,$$

and then:

$$r = \sqrt{x_{bow}^2 + y_{bow}^2}.$$

The force components in global frame are:

$$F_{x,anchor} = -F_{anchor}(r)\,\frac{x_{bow}}{r}, \qquad F_{y,anchor} = -F_{anchor}(r)\,\frac{y_{bow}}{r},$$

with the yaw moment about the COG calculated as:

$$N_{anchor} = F_{y,anchor}\left(\frac{L_{pp}}{2} - x_g\right).$$

These components are transformed into the body frame using transformation matrix:

$$\boldsymbol{\tau}_{anchor} = \boldsymbol{\mathcal{J}}(\psi)\begin{bmatrix} F_{x,anchor} \\ F_{y,anchor} \\ N_{anchor} \end{bmatrix}.$$

Development of the model. Wave (next steps)

- External forces WAVE

$$\tau_{x,wave} = \sum_i A_i RAO_{surge}(\omega_{e,i}, \theta_{r,i}) \cos(\phi_{wave,i} - \phi_{surge,i}) \ ,$$
$$\tau_{y,wave} = \sum_i A_i RAO_{sway}(\omega_{e,i}, \theta_{r,i}) \cos(\phi_{wave,i} - \phi_{sway,i}) \ ,$$

where A_i – amplitude of wave component i, $\phi_{surge/sway,i}$ are RAO phase shifts, and phase of wave i-th component at ship's location is:

$$\phi_{wave,i} = k_i(x_{ship} \cos\theta_i + y_{ship} \sin\theta_i) - \omega_{e,i}t + \phi_i \ ,$$

where k_i – wave number of i-th component derived from dispersion equation, x_{ship}, y_{ship} – ship position in global frame, $\omega_{e,i}$ encounter frequency of wave component i, t – current time, ϕ_i – initial phase of the wave component.

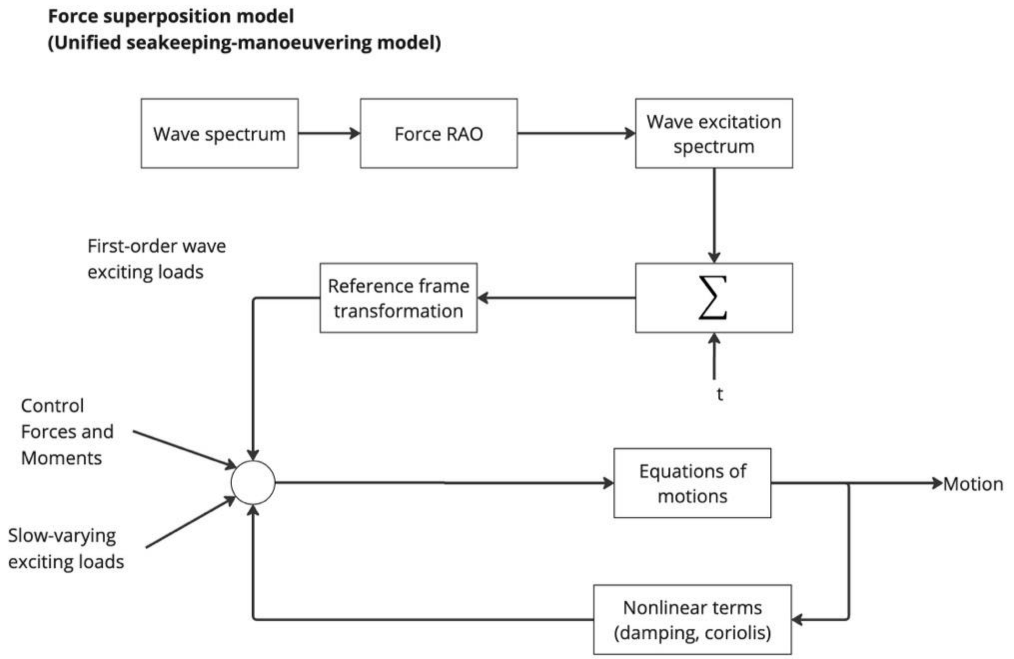

Unified model for maneuvering and seakeeping (adapted from Perez and Fossen 2006).

Not implemented.

Development of the model.
Thrust Allocation (next step)

After computing propulsion **forces** from the control system, these forces must be allocated to individual thrusters.

For a catamaran equipped with two fixed (non-rotatable) thrusters, one on each demihulls, the control outputs include:

- Forward thrust from each thruster (F_{port},F_{star}) generating surge force (τ_x)
- Differential thrust between thrusters controlling the yaw moment (τ_ψ).
- Sway motion (τ_y) cannot be directly generated since the thrusters are fixed in orientation

$$\begin{cases} F_{port} + F_{star} = \tau_x \\ \frac{b}{2} \cdot (F_{port} - F_{star}) = \tau_\psi \end{cases} \Longrightarrow \begin{aligned} F_{port} &= \frac{\tau_x}{2} + \frac{2\tau_\psi}{b} \\ F_{star} &= \frac{\tau_x}{2} - \frac{2\tau_\psi}{b} \end{aligned}$$

Not implemented.

Development of the model

The Delft 372 catamaran (Van’t Veer 1998)

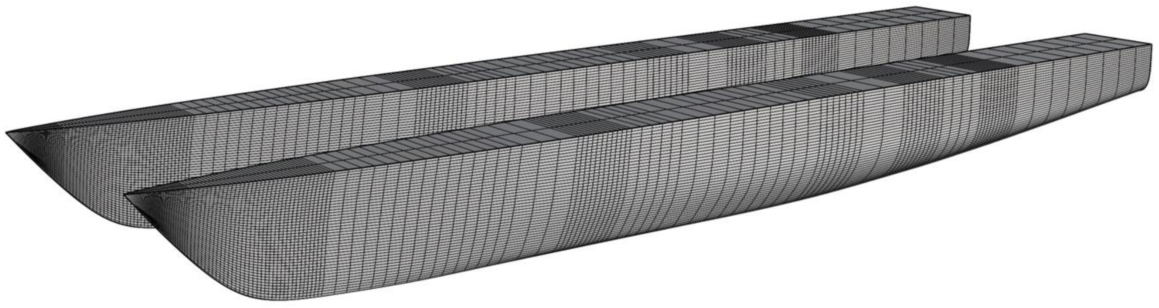

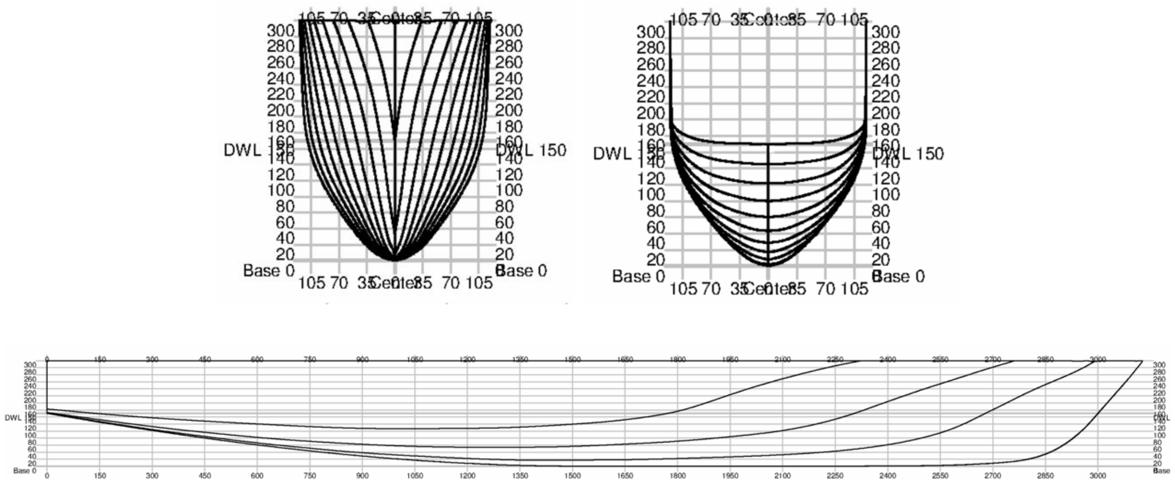

Lines taken from Remmlinger 2014

Parameter	Value	Units	Comments
Displacement	87.07	kg	
Yaw Moment of Inertia	58.9	kg·m²	Derived from geometric Moment of Inertia
Center of Gravity (x-location)	-0.09	m	Relative to the midship
Length between Perpendiculars	3	m	
Lateral Area	1.5	m²	Assumed value
Frontal Area	0.5	m²	Assumed value
Wind Drag Coefficient	0.2	–	Assumed value

Development of the model

(Mai 2020)

- Delft 372 + modification of Damping

한국항해항만학회지 제44권 제2호
J. Navig. Port Res. Vol. 44, No. 2 : 53-64, April 2020 (ISSN:1598-5725(Print)/ISSN:2093-8470(Online))
DOI : http://dx.doi.org/10.5394/KINPR.2020.44.2.53

Analysis on Hydrodynamic Force Acting on a Catamaran at Low Speed Using RANS Numerical Method

Thi Loan Mai · Tien Thua Nguyen** · Myungjun Jeon*** · † Hyeon Kyu Yoon*
,,***Student, Graduate Sschool of Changwon National University, Gyeongsangnam-do, 51140, Korea*
† Professor of Changwon National University, Gyeongsangnam-do, 51140, Korea

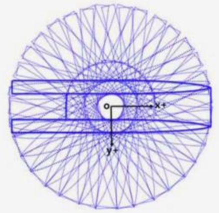

Fig. 4 Pure rotating test

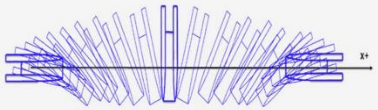

Fig. 5 Yaw rotating test

Table 7 Estimated hydrodynamic coefficients for Delft 372 catamaran at low speed

Coefficient	Values	Coefficient	Values
X'_{uu}	-2.12E-02	N'_{v}	-1.72E-01
X'_{vr}	3.26E-03	N'_{uv}	-1.63E-01
Y'_{v}	-7.60E-01	N'_{vvv}	1.17E-01
Y'_{vvv}	-1.9E+00	N'_{uvvv}	-3.67E-01
Y'_{vvvvv}	1.94E+00	N'_{r}	-4.05E-02
Y'_{ur}	-6.37E-01	$N'_{r\|r\|}$	-8.10E-2
$Y'_{ur\|r\|}$	1.15E+00	$N'_{uv\|r\|}$	2.20E-01
$Y'_{v\|r\|}$	-5.22E-01	N'_{vvr}	8.10E-02
$Y'_{\dot{v}}$	-1.33E-01	$N'_{\dot{v}}$	1.42E-02
$Y'_{\dot{r}}$	6.07E-04	$N'_{\dot{r}}$	-2.96E-02

The original dimensionless values were obtained using the Prime 2 system with Fn = 0.06. For current study they are converted back to dimensional form.

$$X'_H = X'_{uu}u'^2 + X'_{vr}v'r'$$
$$Y'_H = Y'_v v' + Y'_{vvv}v'^3 + Y'_{vvvvv}v'^5 + Y'_{ur}u'r' + Y'_{v|r|}v'|r'| + Y'_{ur|r|}u'r'|r'|$$
$$N'_H = N'_v v' + N'_{uv}u'v' + N'_{vvv}v'^3 + N'_{uvvv}u'v'^3 + N'_r r' + N'_{r|r|}r'|r'| + N'_{uv|r|}u'v'|r'| + N'_{vv|r|}v'^2|r|$$

Standard Fossen:

$$\boldsymbol{D}_{NL} = -\begin{bmatrix} X_{|u|u}|u_r| & 0 & 0 \\ 0 & Y_{|v|v}|v_r| + Y_{|r|v}|r| & Y_{|v|r}|v_r| + Y_{|r|r}|r| \\ 0 & N_{|v|v}|v_r| + N_{|r|v}r & N_{|v|r}|v| + N_{|r|r}|r| \end{bmatrix}$$

Development of the model

(Mai 2020)

- Delft 372 + modification of Damping

한국항해항만학회지 제44권 제2호
J. Navig. Port Res. Vol. 44, No. 2 : 53-64, April 2020 (ISSN:1598-5725(Print)/ISSN:2093-8470(Online))
DOI : http://dx.doi.org/10.5394/KINPR.2020.44.2.53

Analysis on Hydrodynamic Force Acting on a Catamaran at Low Speed Using RANS Numerical Method

Thi Loan Mai · Tien Thua Nguyen** · Myungjun Jeon*** · † Hyeon Kyu Yoon*
,,***Student, Graduate Sschool of Changwon National University, Gyeongsangnam-do, 51140, Korea*
† Professor of Changwon National University, Gyeongsangnam-do, 51140, Korea

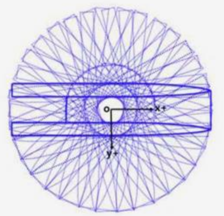

Fig. 4 Pure rotating test

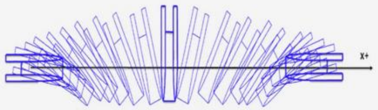

Fig. 5 Yaw rotating test

Table 7 Estimated hydrodynamic coefficients for Delft 372 catamaran at low speed

Coefficient	Values	Coefficient	Values
X'_{uu}	-2.12E-02	N'_{v}	-1.72E-01
X'_{vr}	3.26E-03	N'_{uv}	-1.63E-01
Y'_{v}	-7.60E-01	N'_{vvv}	1.17E-01
Y'_{vvv}	-1.9E+00	N'_{uvvv}	-3.67E-01
Y'_{vvvvv}	1.94E+00	N'_{r}	-4.05E-02
Y'_{ur}	-6.37E-01	$N'_{r\|r\|}$	-8.10E-2
$Y'_{ur\|r\|}$	1.15E+00	$N'_{uv\|r\|}$	2.20E-01
$Y'_{v\|r\|}$	-5.22E-01	N'_{vvr}	8.10E-02
$Y'_{\dot{v}}$	-1.33E-01	$N'_{\dot{v}}$	1.42E-02
$Y'_{\dot{r}}$	6.07E-04	$N'_{\dot{r}}$	-2.96E-02

The original dimensionless values were obtained using the Prime 2 system with Fn = 0.06. For current study they are converted back to dimensional form.

$$X'_H = X'_{uu}u'^2 + X'_{vr}v'r'$$
$$Y'_H = Y'_v v' + Y'_{vvv}v'^3 + Y'_{vvvvv}v'^5 + Y'_{ur}u'r' + Y'_{v|r|}v'|r'| + Y'_{ur|r|}u'r'|r'|$$
$$N'_H = N'_v v' + N'_{uv}u'v' + N'_{vvv}v'^3 + N'_{uvvv}u'v'^3 + N'_r r' + N'_{r|r|}r'|r'| + N'_{uv|r|}u'v'|r'| + N'_{vv|r|}v'^2|r|$$

Standard Fossen:

$$\boldsymbol{D}_{NL} = -\begin{bmatrix} X_{|u|u}|u_r| & 0 & 0 \\ 0 & Y_{|v|v}|v_r| + Y_{|r|v}|r| & Y_{|v|r}|v_r| + Y_{|r|r}|r| \\ 0 & N_{|v|v}|v_r| + N_{|r|v}r & N_{|v|r}|v| + N_{|r|r}|r| \end{bmatrix}$$

Modified:

$$\boldsymbol{D}_{NL} = -\begin{bmatrix} X_{uu}u_r & 0 & X_{vr}v_r \\ 0 & Y_{vvv}v_r^2 + Y_{vvvvv}v_r^4 + Y_{vr}|r| & Y_{ur}u_r + Y_{urr}u_r r|r| \\ N_{uv}v_r + N_{uvvv}v_r^3 + N_{uvr}v_r|r| & N_{vvv}v_r^2 + N_{vvr}v_r|r| & N_{rr}|r| \end{bmatrix}$$

Final model

$$\boldsymbol{M}_{RB}\dot{\boldsymbol{\nu}} + \boldsymbol{C}_{RB}(\boldsymbol{\nu})\boldsymbol{\nu} + \boldsymbol{M}_A\dot{\boldsymbol{\nu}}_r + \boldsymbol{C}_A(\boldsymbol{\nu}_r)\boldsymbol{\nu}_r + \boldsymbol{D}(\boldsymbol{\nu}_r)\boldsymbol{\nu}_r = \boldsymbol{\tau}_{prop} + \boldsymbol{\tau}_{anch} + \boldsymbol{\tau}_{wind} + \overset{omitted}{\cancel{\boldsymbol{\tau}_{wave}}}$$

Current

$$\boldsymbol{\nu_r} = \boldsymbol{\nu} - \boldsymbol{\nu_c^b},$$

$$\boldsymbol{\nu}_c^b = [u_c^b, v_c^b, 0]$$

$$\begin{bmatrix} u_c^b \\ v_c^b \end{bmatrix} = \begin{bmatrix} U_{cx}^g \cos\psi + U_{cy}^g \sin\psi \\ -U_{cx}^g \sin\psi + U_{cy}^g \cos\psi \end{bmatrix}$$

$$U_{cx}^g = U_c \cos\beta$$
$$U_{cy}^g = U_c \sin\beta$$

Anchor

$$\boldsymbol{\tau}_{anchor} = \boldsymbol{\mathcal{J}}(\psi) \begin{bmatrix} F_{x,anchor} \\ F_{y,anchor} \\ N_{anchor} \end{bmatrix}$$

$$F_{x,anchor} = -F_{anchor}(r)\,\frac{x_{bow}}{r}$$

$$F_{y,anchor} = -F_{anchor}(r)\,\frac{y_{bow}}{r}$$

$$N_{anchor} = F_{y,anchor}\left(\frac{L_{pp}}{2} - x_g\right)$$

$$F_{anchor}(r) = p(r - r_0)^q$$

Wind

$$\tau_{wind,surge} = 0.5\rho_{air}U_{rel}^2\, C_{d,surge}(\gamma)A_{fr}$$
$$\tau_{wind,sway} = 0.5\rho_{air}U_{rel}^2\, C_{d,sway}(\gamma)A_{lat}$$
$$\tau_{wind,yaw} = 0.5\rho_{air}U_{rel}^2\, C_{d,yaw}(\gamma)A_{lat}L_{pp}$$

$$u_{rel} = u - U_{wind}\,cos(\beta_{wind} - \psi),$$

$$v_{rel} = v - U_{wind}\,sin(\beta_{wind} - \psi),$$

$$U_{rel} = \sqrt{u_{rel}^2 + v_{rel}^2}\,.$$

Modified Non-linear Damping

$$\boldsymbol{D}_{NL} = -\begin{bmatrix} X_{uu}u_r & 0 & X_{vr}v_r \\ 0 & Y_{vvv}v_r^2 + Y_{vvvvv}v_r^4 + Y_{vr}|r| & Y_{ur}u_r + Y_{urr}u_r r|r| \\ N_{uv}v_r + N_{uvvv}v_r^3 + N_{uvr}v_r|r| & N_{vvv}v_r^2 + N_{vvr}v_r|r| & N_{rr}|r| \end{bmatrix}$$

a) 3 DoF
b) No Waves
c) No Thrust Allocation
d) Simplified anchor line dynamic (power-law)
c) Delft 372 – specific Hydrodynamic coefficients

Implementation – block diagram

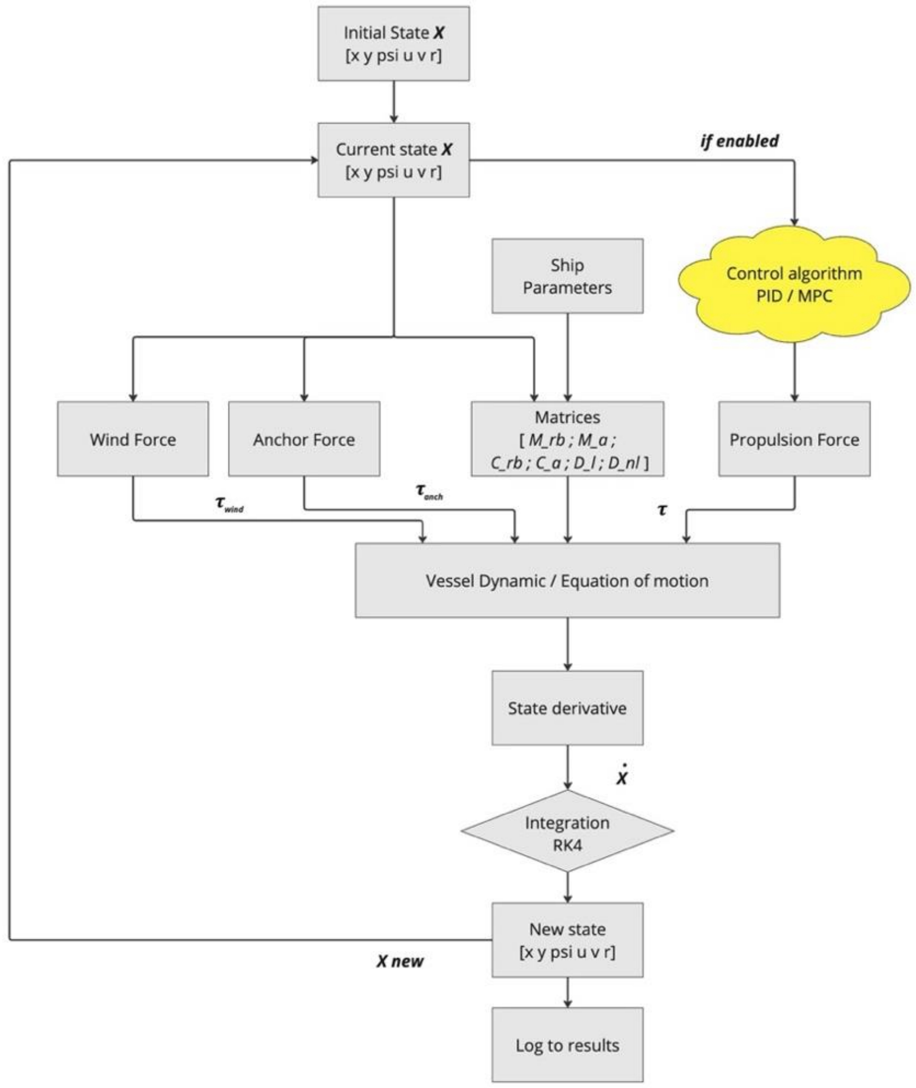


```
...
  FOR t FROM 0 TO t_max STEP dt DO

      // 1. Compute environmental forces
      COMPUTE wind_force
      COMPUTE current effects (transform global current to ship body frame)

      // 2. Compute anchor force using power-law model
      COMPUTE anchor_force and its magnitude

      // 3. Determine control action if enabled
      COMPUTE control_force ← controller (current state, measured forces)

      // 4. Sum all external forces
      SET total_force ← wind_force + anchor_force + control_force

      // 5. Integrate system dynamics
      COMPUTE state_derivative using dynamic equations with total_force
      UPDATE state using RK4 integration method

      // 6. Log simulation data (time, state, forces, etc.)
      STORE current simulation data

  END FOR

  // 7. Post-Processing
  GENERATE summary metrics and plots

END SIMULATION
```

time step = 0.1 sec
simulation time ≥ 600 sec

Simulation Scenarios

A. No Wind
B. No Current
C. Wind and Current variants
D. Angle variance Wind and Current

and Control separately

A) NW – No Wind

ID	Wind (m/s)	Current (m/s)
NW1	0	0.1
NW2	0	0.15
NW3	0	0.2
NW4	0	0.25
NW5	0	0.3
NW6	0	0.35
NW7 *	**0**	**0.4**
NW8	0	0.45
NW9	0	0.48

B) NC – No Current

ID	Wind (m/s)	Current (m/s)
NC1	2	0
NC2	4	0
NC3	6	0
NC4	8	0
NC5	10	0
NC6	12	0
NC7	14	0
NC8	16	0

C) CW –Wind & Current

ID	Wind (m/s)	Current (m/s)	ID	Wind (m/s)	Current (m/s)
CWA1	6	0.01	CWD1	14	0
CWA2	6	0.1	CWD2	14	0.2
CWA3	6	0.2	CWD3	14	0.3
CWA4	6	0.3	CWD4	14	0.4
CWB1	10	0.01	CWE1	18	0.15
CWB2	10	0.1	CWE2	18	0.2
CWB3	10	0.2	CWE3	18	0.3
CWB4	10	0.3	CWE4	18	0.4
			CWE5	18	0.45
CWC1	12	0			
CWC2	12	0.2			
CWC3	12	0.3			
CWC4	12	0.4			

D) ACW – Angle Variance

ID	Wind (m/s)	Current (m/s)	Relative Angle		ID	Wind (m/s)	Current (m/s)	Relative Angle
ACW1	14	0.4	0		ACW5	14	0.4	30
ACW2	14	0.4	10		ACW6	14	0.4	45
ACW3	14	0.4	15		ACW7	14	0.4	60
ACW3	14	0.4	20		ACW8	14	0.4	90
ACW4	14	0.4	25		ACW4B	14	0.2	25
					ACW4C	14	0.3	25

A) No Wind

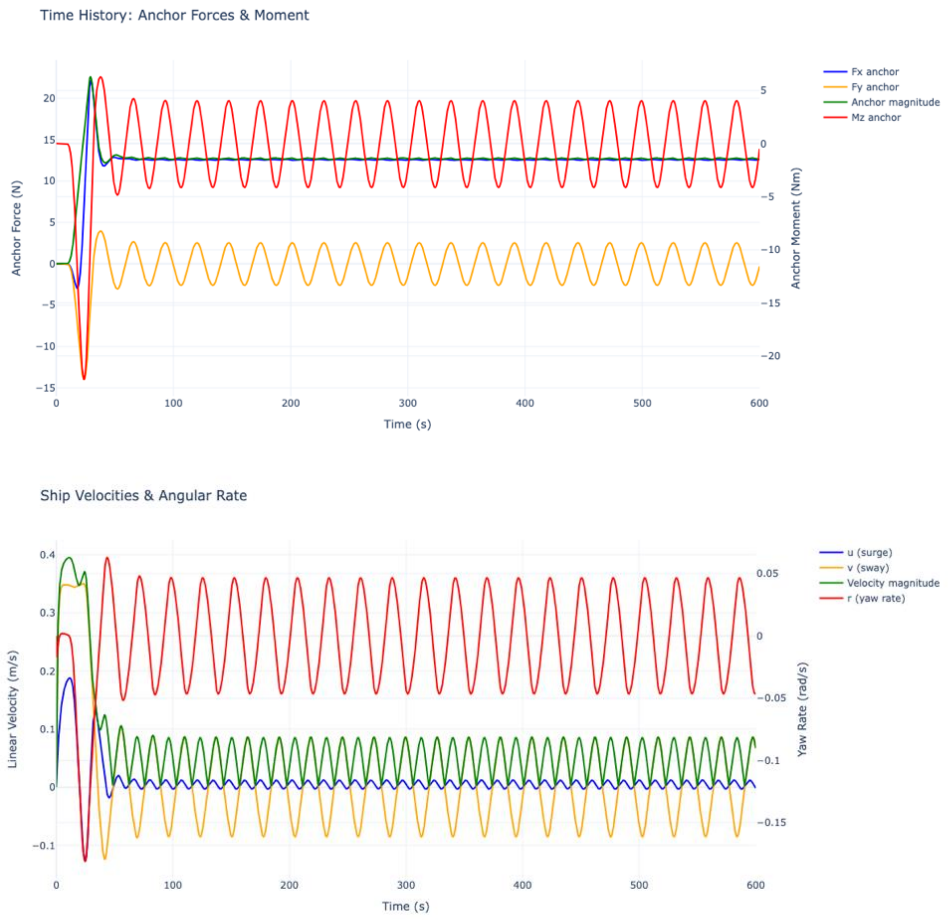

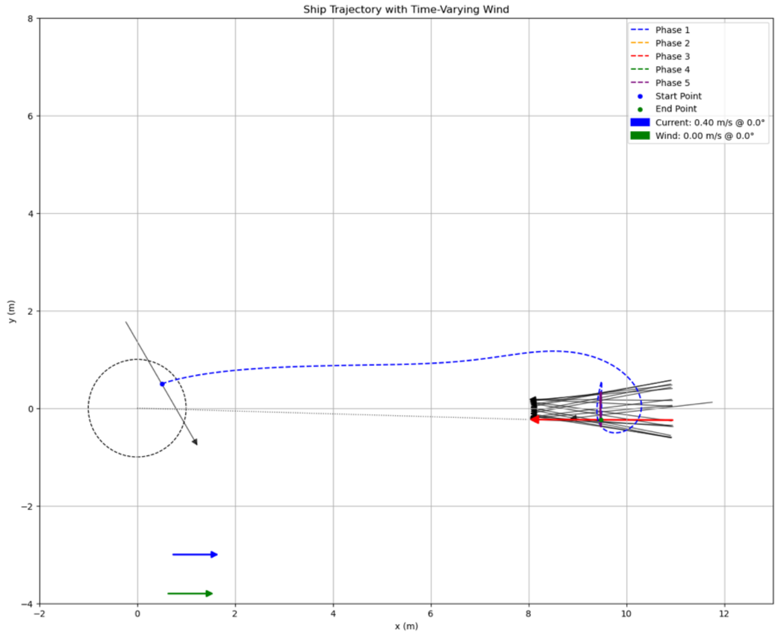

NW7 Case (No Wind, Current = 0.4 m/s).

Blue and green arrows indicate the directions of the current and wind.
Red arrow marks the vessel's end position.

A) No Wind

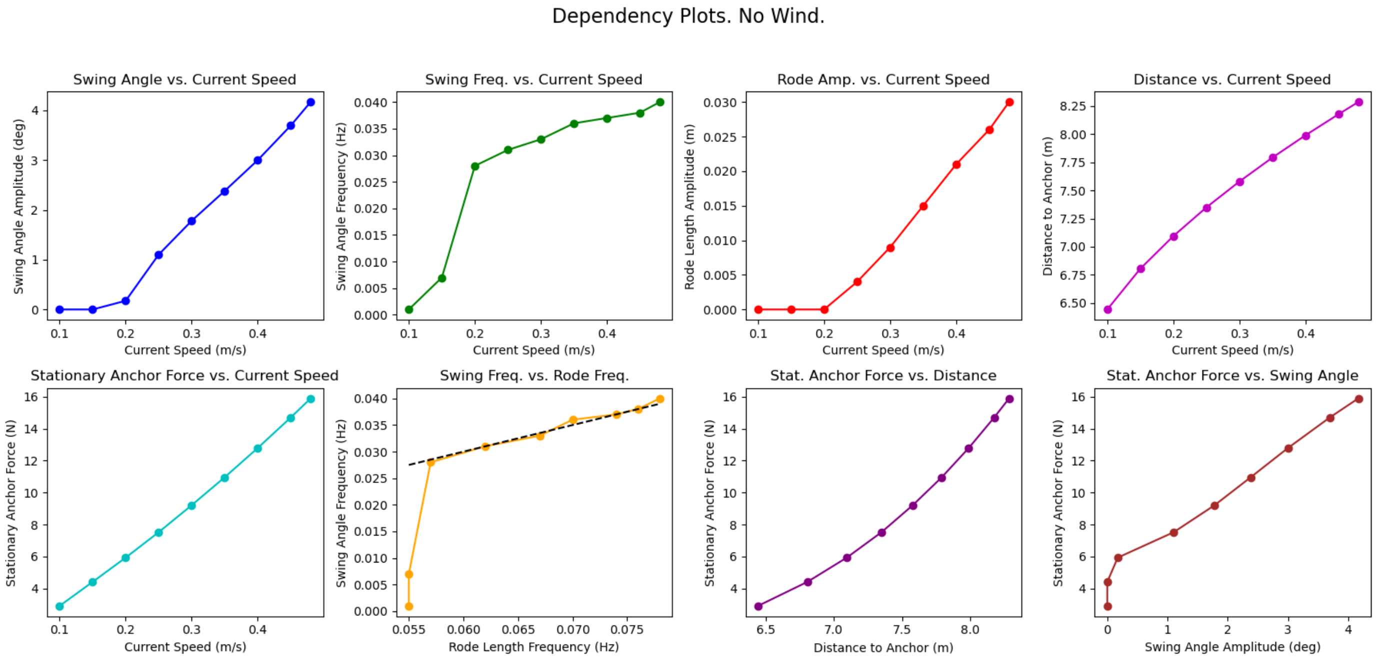

A) NW – No Wind		
ID	**Wind (m/s)**	**Current (m/s)**
NW1	0	0.1
NW2	0	0.15
NW3	0	0.2
NW4	0	0.25
NW5	0	0.3
NW6	0	0.35
NW7 *	**0**	**0.4**
NW8	0	0.45
NW9	0	0.48

- At low Velocities - no oscillations
- Swing increases with Current Speed
- Though amplitude of Swing oscillations is not big (previous slide)
- Small oscillations also in surge direction
- Anchor line tension has linear dependance

B) No Current

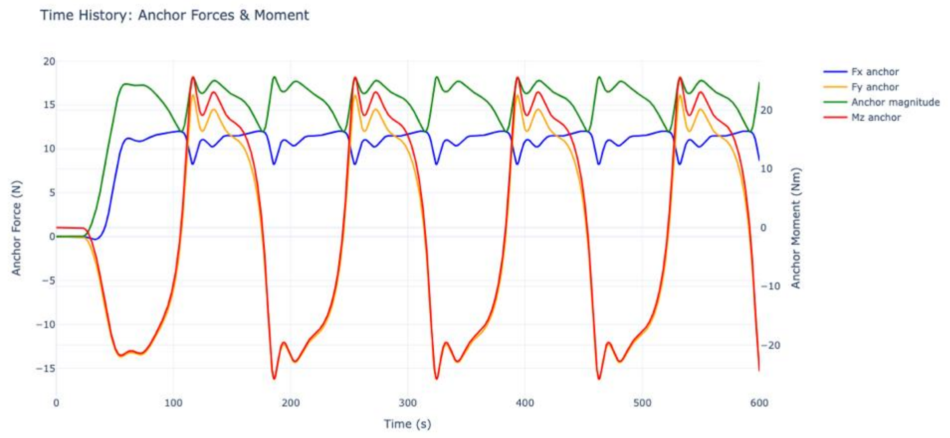

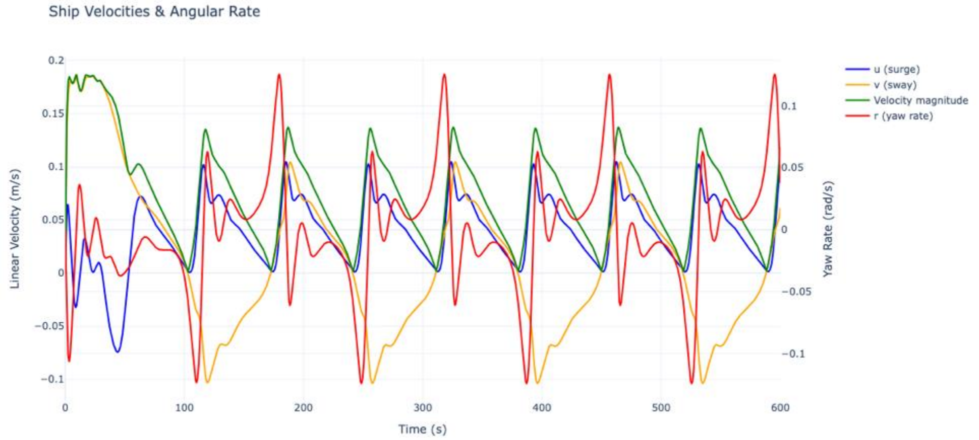

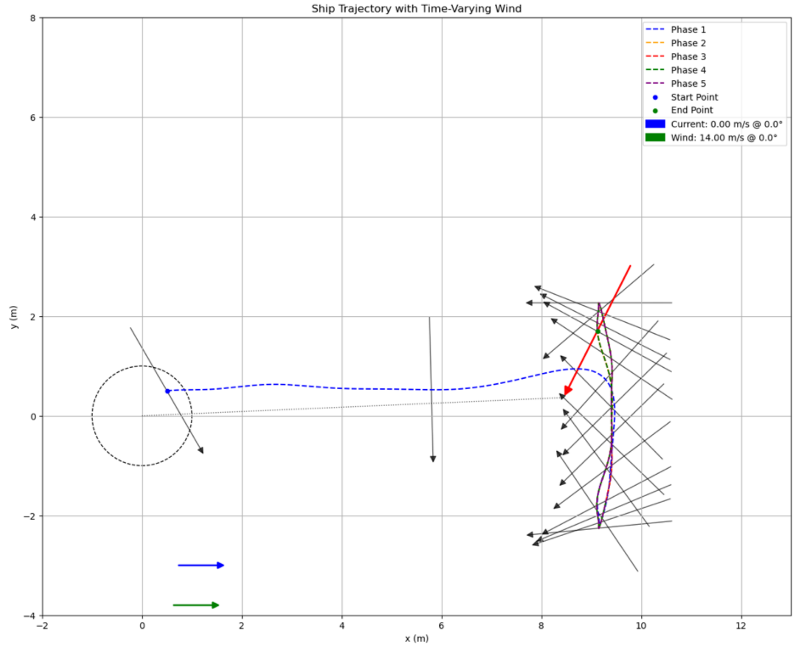

NC7 Case (No Current, Wind = 14 m/s).

Blue and green arrows indicate the directions of the current and wind.
Red arrow marks the vessel's end position.

B) No Current

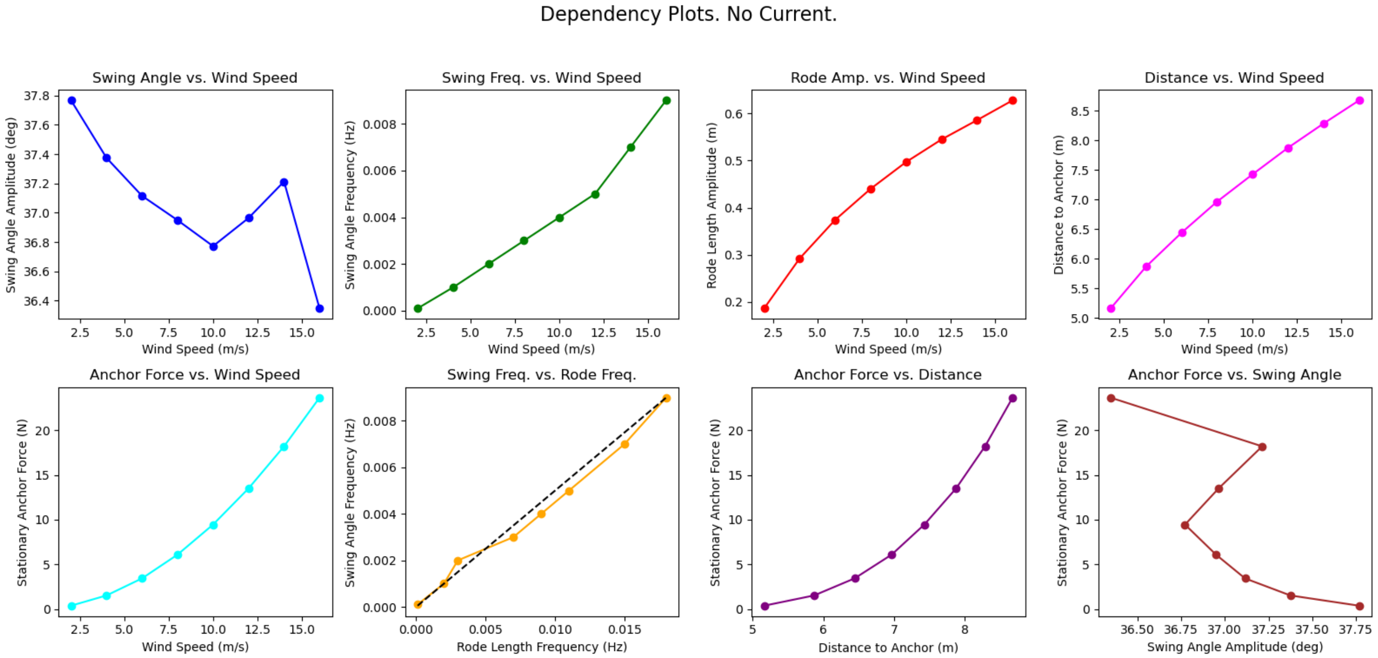

B) NC – No Current		
ID	**Wind (m/s)**	**Current (m/s)**
NC1	2	0
NC2	4	0
NC3	6	0
NC4	8	0
NC5	10	0
NC6	12	0
NC7 *	**14**	**0**
NC8	16	0

- Oscillations present even for small Wind Speed
- Swing amplitude does not depend on Speed (but frequency)
- Frequencies of oscillations are lower than in NW scenarios
- Swing amplitude is big for the whole range
- Pattern is not regular (previous slide)
- Anchor line tension – non linear dependance

C) Wind and Current variants

- Constant Current with Varying Wind speed (same direction)

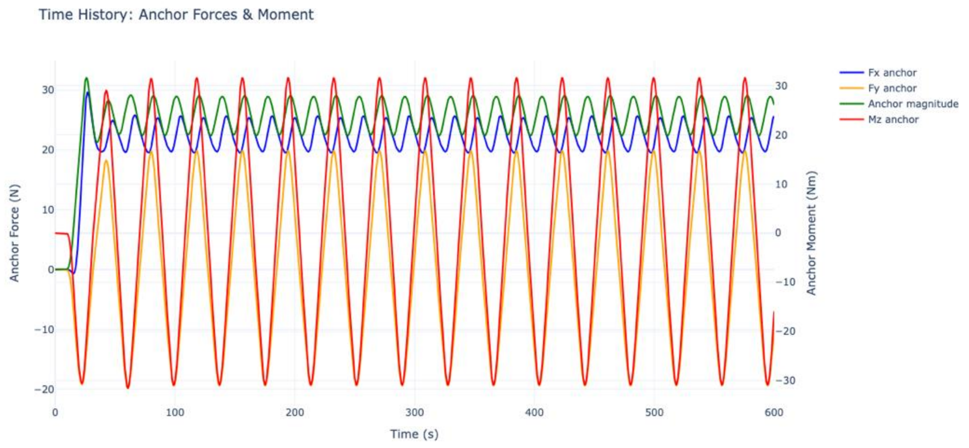

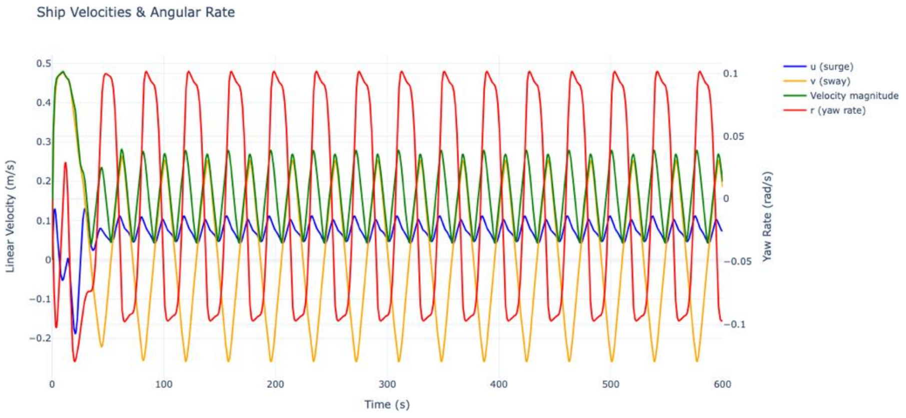

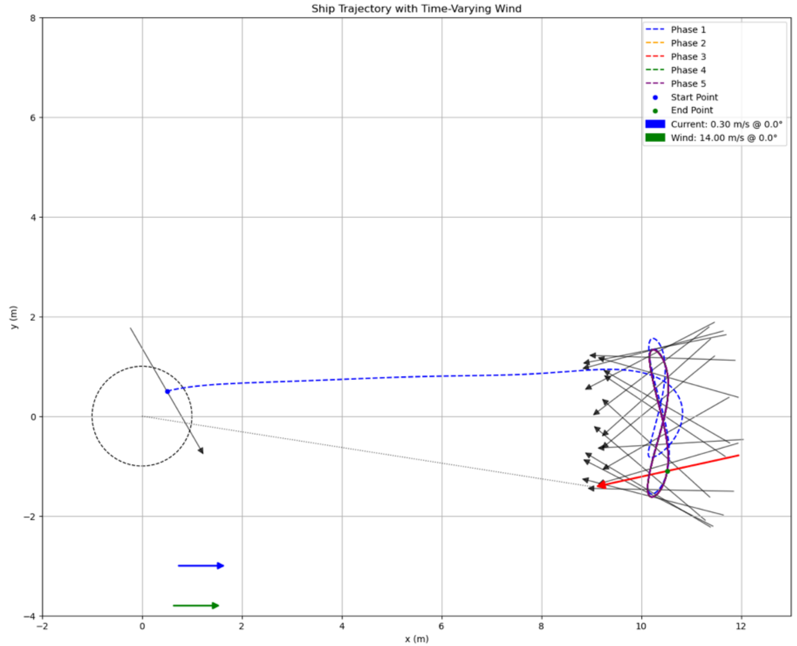

CWD3 Case (Wind = 14 m/s, Current = 0.3 m/s)

C) Wind and Current variants

- Constant Current with Varying Wind speed (same direction)

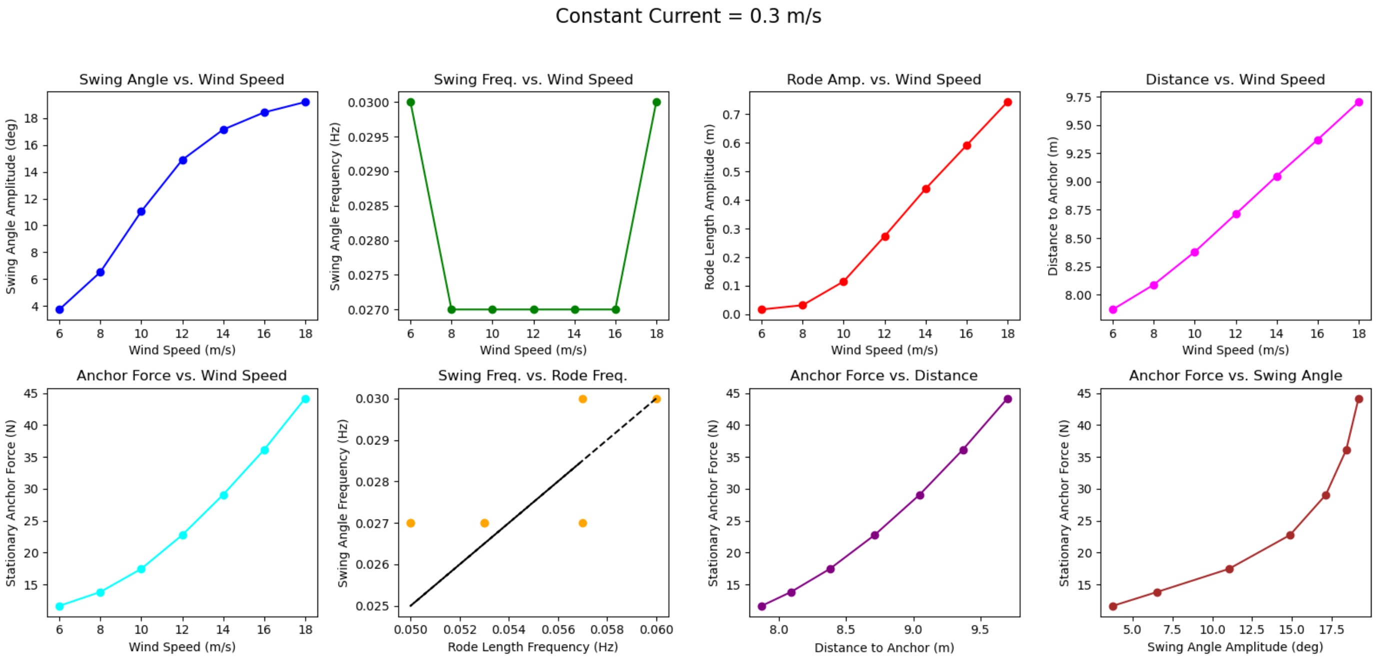

- Wind is major factor for swinging
- Swing Frequency is almost constant and comparable to NW series
- Emergence of ”eight” pattern (previous slide)

C) CW –Wind & Current

ID	Wind (m/s)	Current (m/s)	ID	Wind (m/s)	Current (m/s)
CWA1	6	0.01	CWD1	14	0
CWA2	6	0.1	CWD2	14	0.2
CWA3	6	0.2	**CWD3 ****	**14**	**0.3**
CWA4 *	**6**	**0.3**	CWD4	14	0.4
CWB1	10	0.01	CWE1	18	0.15
CWB2	10	0.1	CWE2	18	0.2
CWB3	10	0.2	**CWE3 ***	**18**	**0.3**
CWB4 *	**10**	**0.3**	CWE4	18	0.4
			CWE5	18	0.45
CWC1	12	0			
CWC2	12	0.2			
CWC3 *	**12**	**0.3**			
CWC4	12	0.4			

C) Wind and Current variants

- Constant Wind with Varying Current speed (same direction)

- Current stabilizes swing oscillations
- Anchor line tension depends linearly from Current
- Frequencies of swinging and surging are ”coupled”
- Anchor line tension follows power law (deviance because max tension is plotted)

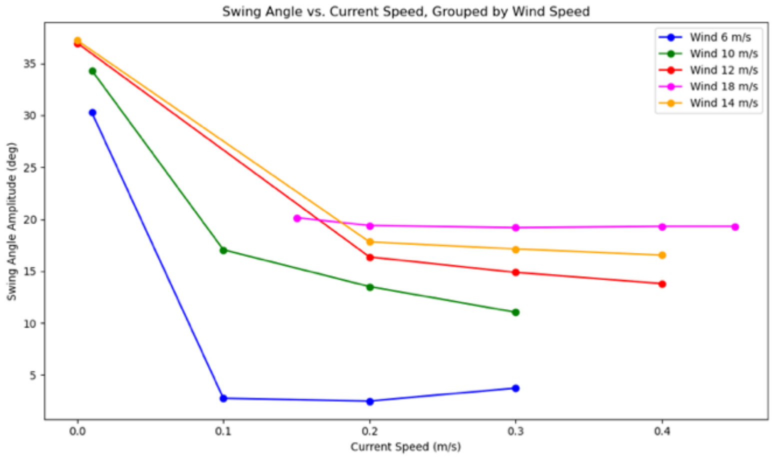

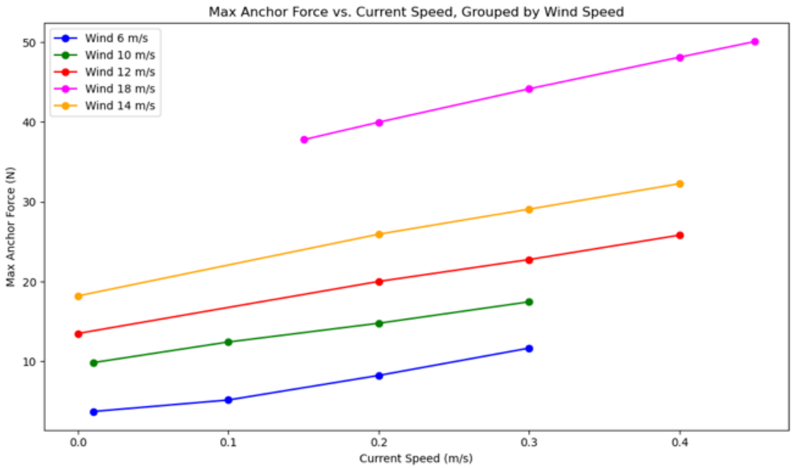

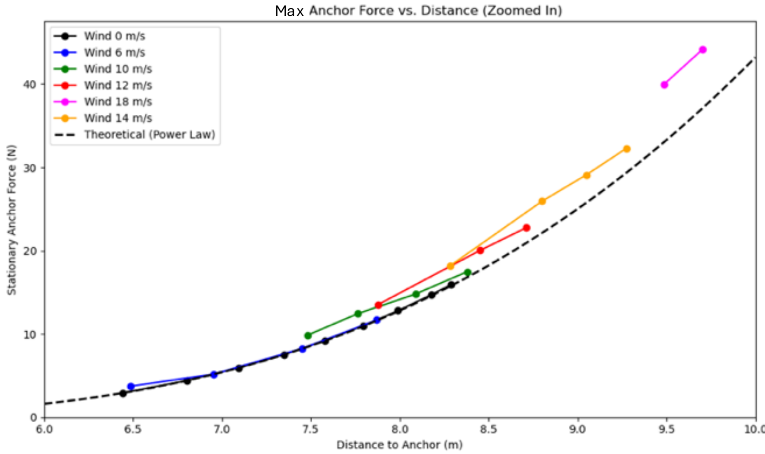

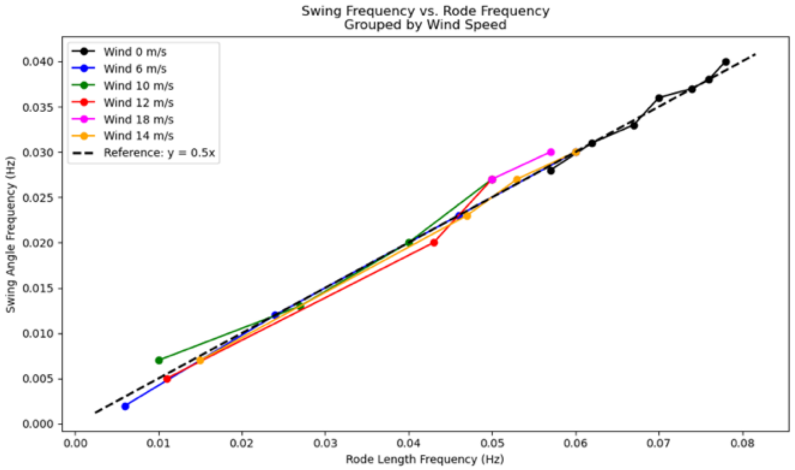

D) Constant Wind and Current with Varying Relative Angle

- Less swinging amplitude with bigger angle
- At 90 deg misalignment Anchor Line tension is minimal
- Nonsignificant increase of swing amplitude at 90 deg

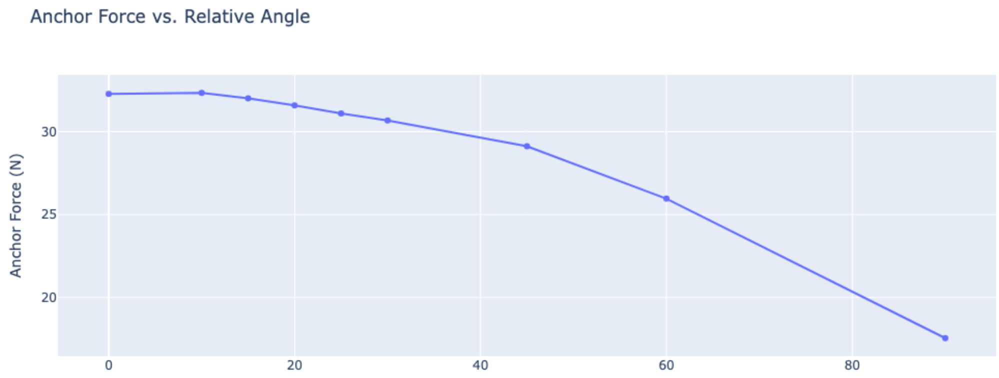

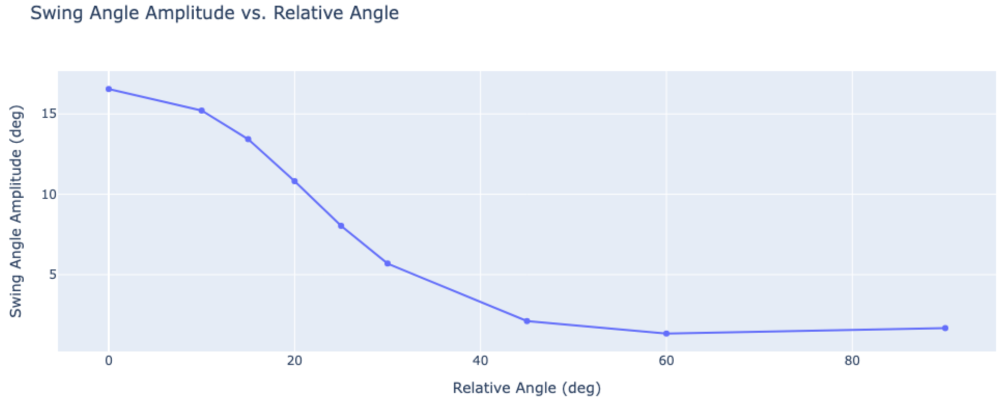

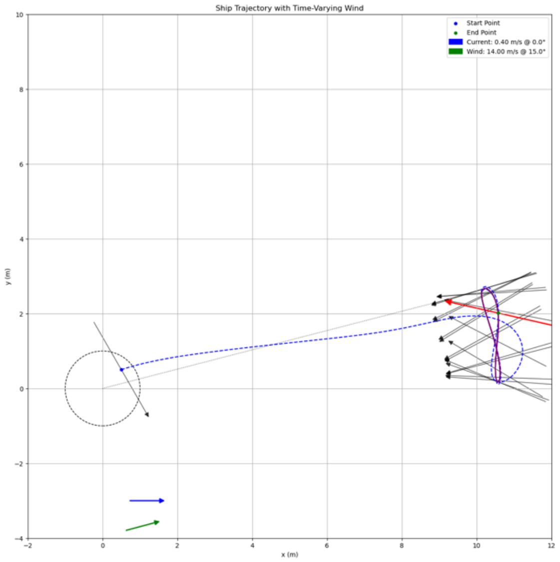

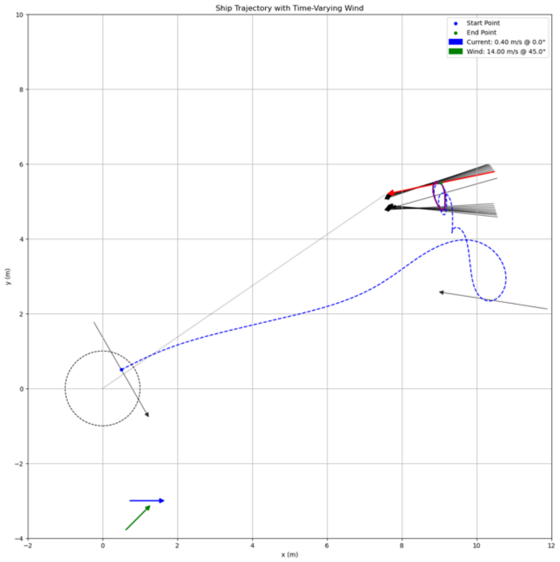

D) ACW – Angle Variance								
ID	Wind (m/s)	Current (m/s)	Relative Angle		ID	Wind (m/s)	Current (m/s)	Relative Angle
ACW1	14	0.4	0		ACW5	14	0.4	30
ACW2	14	0.4	10		ACW6	14	0.4	45
ACW3	14	0.4	15		ACW7	14	0.4	60
ACW3	14	0.4	20		ACW8	14	0.4	90
ACW4	14	0.4	25		ACW4B	14	0.2	25
					ACW4C	14	0.3	25

Control

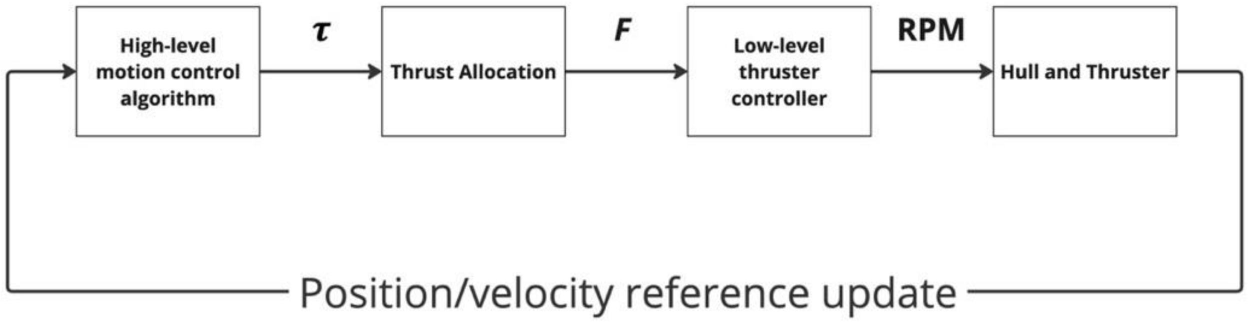

1. Model Predictive Controller (MPC)

Prediction of future state and optimization

2. Proportional-Derivative (PD)

Reactive feedback
Sway and Yaw velocities setpoints

Control algorithms. PD

Control Objective: Minimize lateral movement

$$\tau_y = K_{y,p}(v_d - v) + K_{y,d}\frac{d}{dt}(v_d - v)$$

$$\tau_\psi = K_{\psi,p}(r_d - r) + K_{\psi,d}\frac{d}{dt}(r_d - r)$$

$$\Delta\tau = \max(-\mathrm{rate}_{\max} \cdot dt, \min(\tau_{desired} - \tau_{prev}, \mathrm{rate}_{\max} \cdot dt)).$$

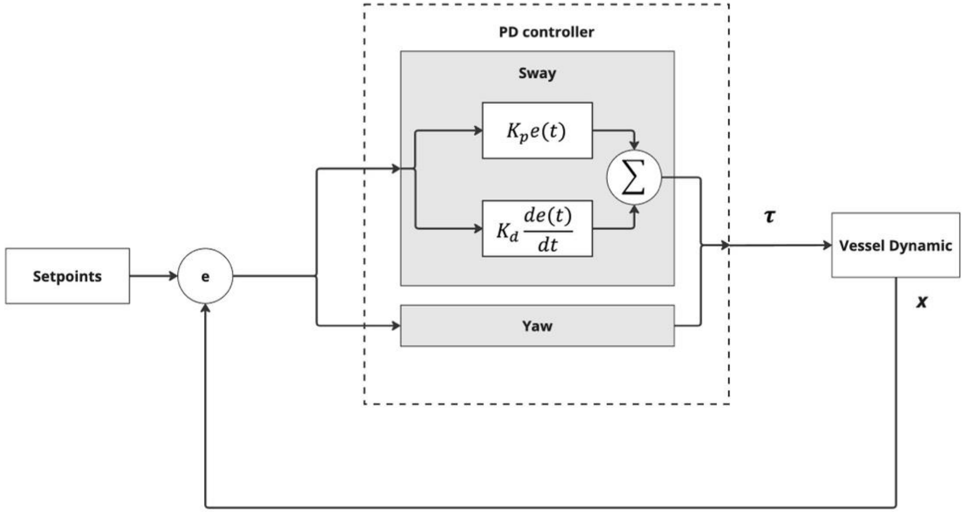

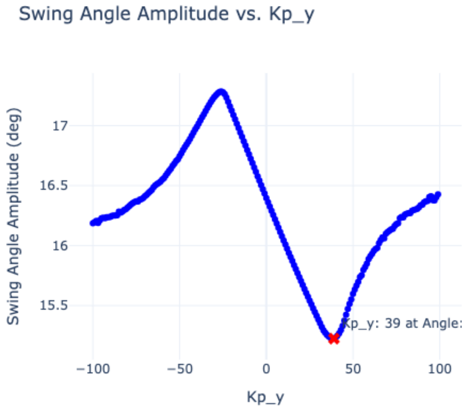

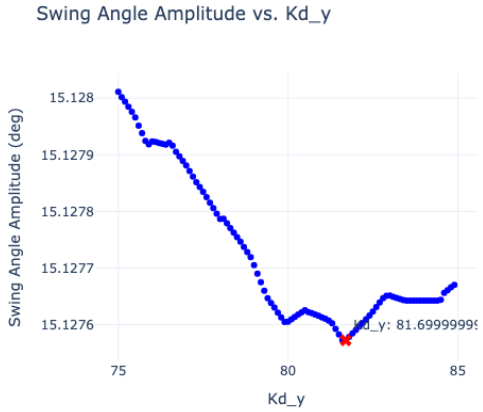

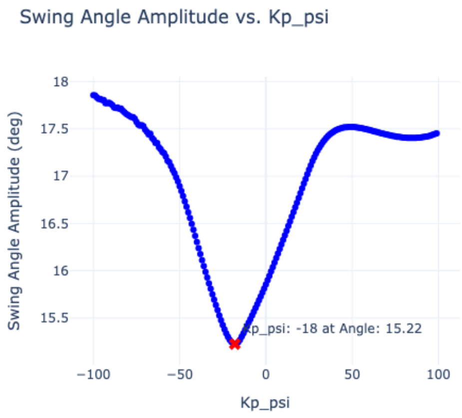

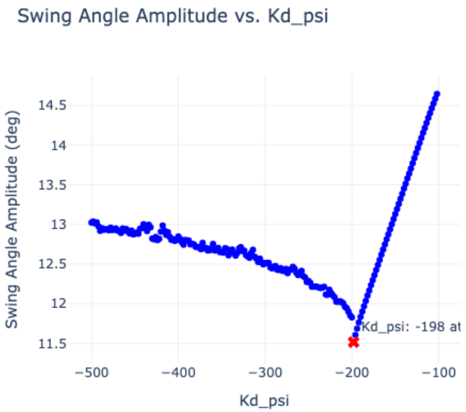

Model Predictive Control

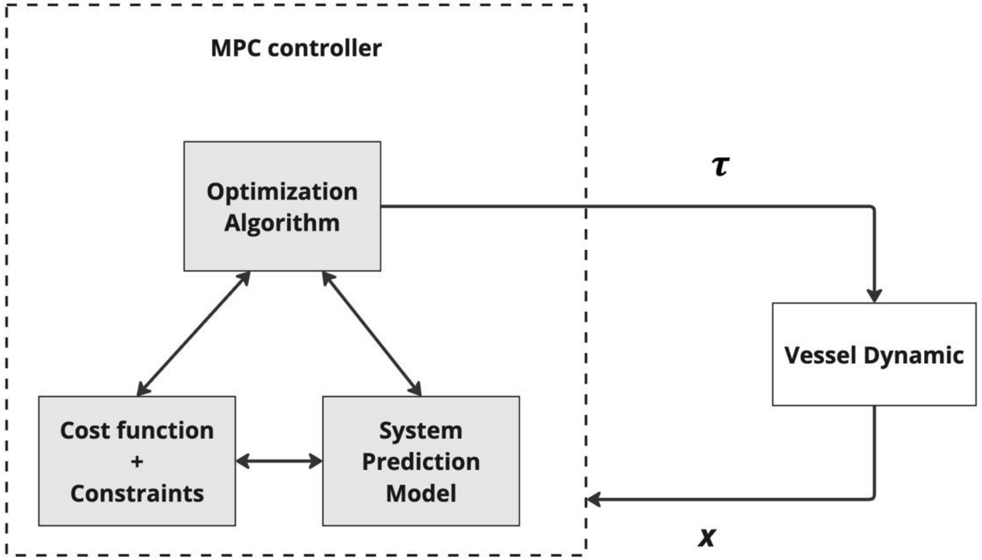

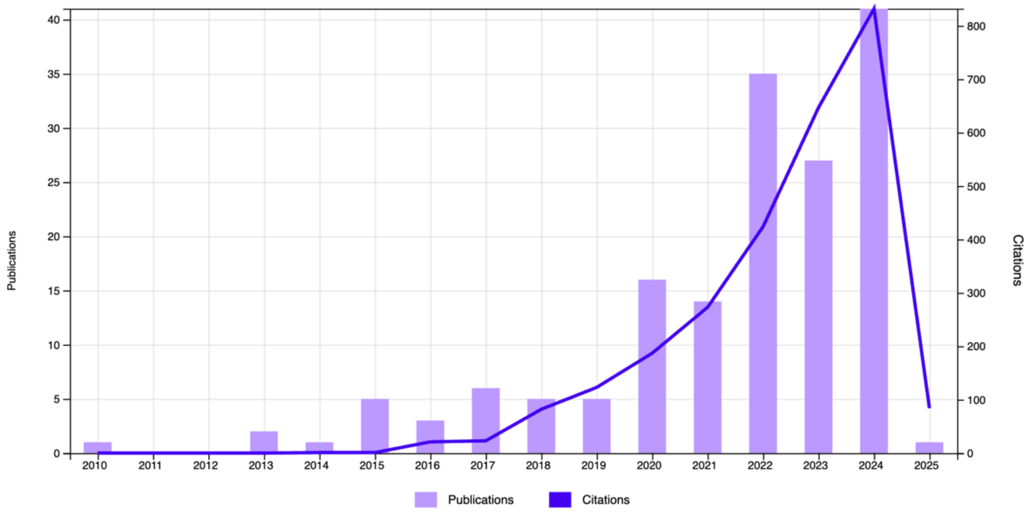

query: ("model predictive control" OR MPC) AND ("autonomous marine vessels" OR AMV OR "autonomous maritime vessels" OR "autonomous ships" OR "unmanned surface vehicles" OR USV OR "unmanned maritime systems" OR "maritime drones") NOT (automotive OR aerospace OR "industrial automation").

Model Predictive Control

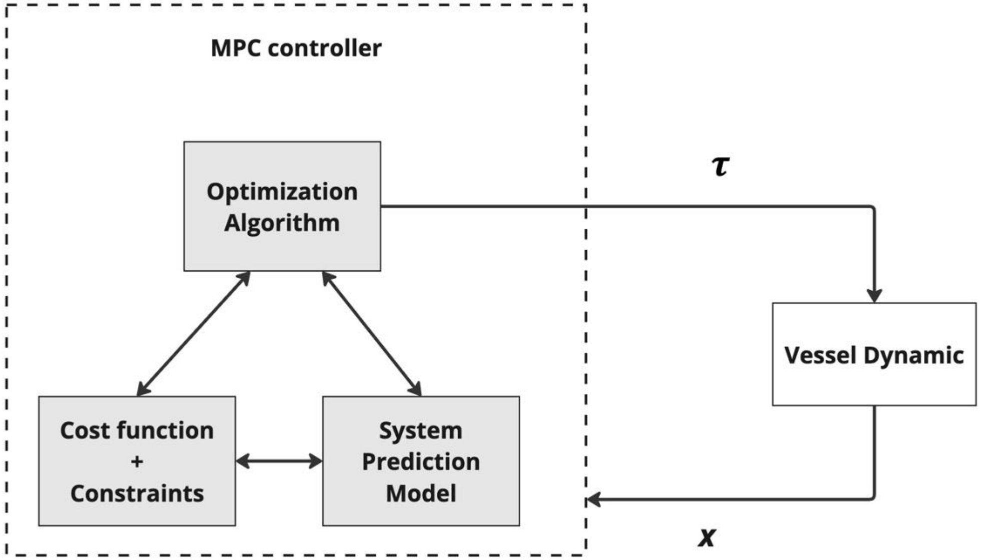

Realized with CasADi and do-mpc python libraries

$$\boldsymbol{x} = [\boldsymbol{\eta} \quad \boldsymbol{\nu}]^T = [x \quad y \quad \psi \quad u \quad v \quad r]^T.$$

$$L_{stage}(\boldsymbol{\nu}, \boldsymbol{\eta}, \boldsymbol{\tau}) = \boldsymbol{\nu}^T \boldsymbol{Q}_{\nu} \boldsymbol{\nu} + \boldsymbol{\eta}^T \boldsymbol{Q}_{\eta} \boldsymbol{\eta} + \boldsymbol{\tau}^T \boldsymbol{Q}_{\tau} \boldsymbol{\tau}$$

$$L_{terminal}(\boldsymbol{\eta}, \boldsymbol{\nu}) = \boldsymbol{\nu}^T \boldsymbol{Q}_{\nu}^{term} \boldsymbol{\nu} + \boldsymbol{\eta}^T \boldsymbol{Q}_{\eta}^{term} \boldsymbol{\eta}$$

$$\min_{\{\boldsymbol{\tau}_{k+j}\}_{j=0}^{N-1}} \sum_{j=0}^{N-1} L_{stage}(\boldsymbol{\nu}_{k+j}, \boldsymbol{\eta}_{k+j}, \boldsymbol{\tau}_{k+j}) + L_{term}(\boldsymbol{\nu}_{k+j}, \boldsymbol{\eta}_{k+j})$$

$$\text{subject to} \quad \begin{cases} \boldsymbol{x}_{k+1} = f(\boldsymbol{x}_k, \boldsymbol{\tau_k}), & (dynamics), \\ \tau_{min} \leq \boldsymbol{\tau} \leq \tau_{max}, & (input\ bounds), \\ |\tau_{k+1} - \tau_k| \leq \Delta\tau, & (rate\ limits). \end{cases}$$

Energy estimation

$$F_{trans} = \sqrt{F_x^2 + F_y^2}$$

$$M_z = (F \cdot \frac{L_{pp}}{2})$$

$$F_z = \frac{M_z}{L_{pp}}$$

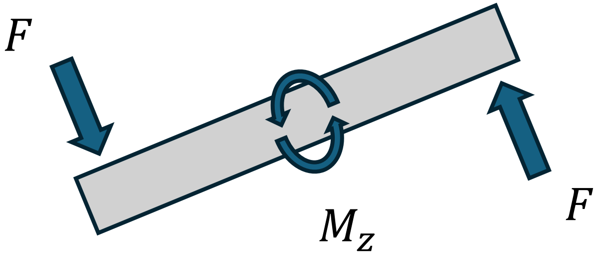

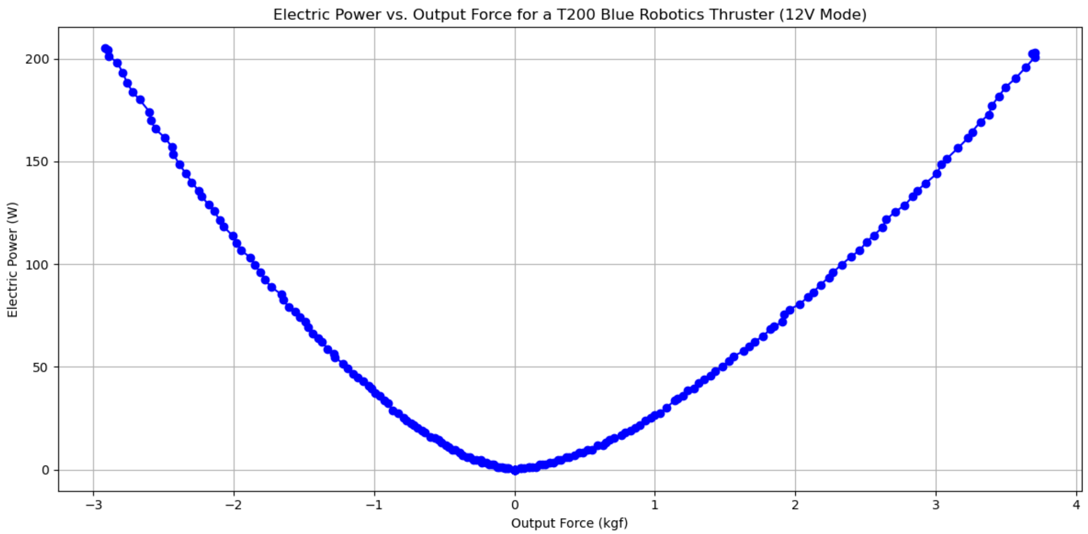

Electric Power vs. Output Force for a T200 Blue Robotics Thruster in 12V Mode.

$$P = f(F)$$

$$P_{total} = P_{trans} + P_z \quad \text{(W)}$$

Control Results. MPC. a)

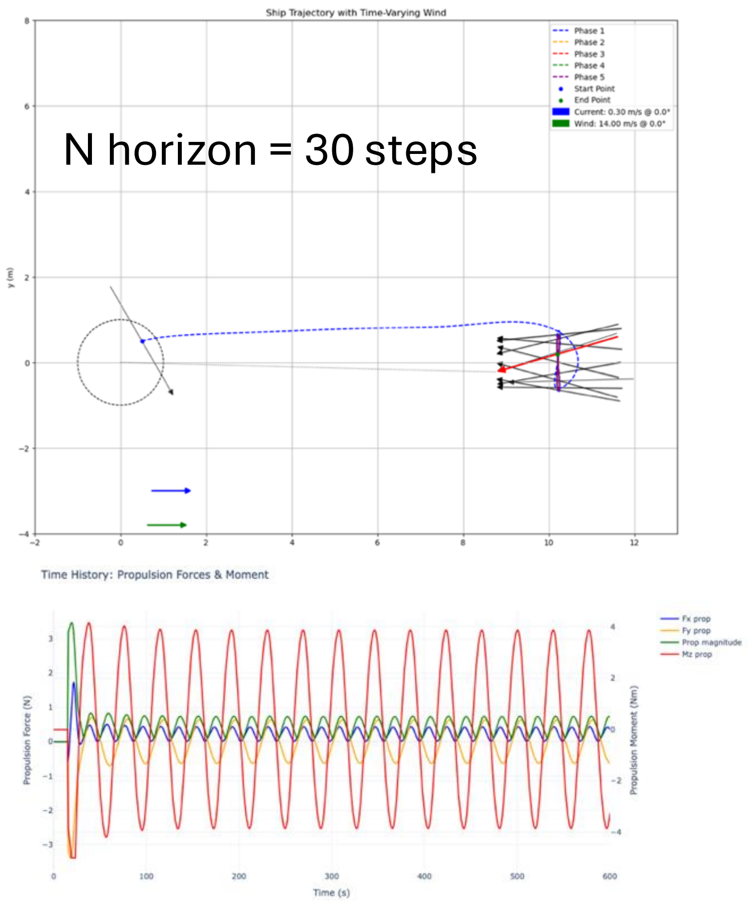

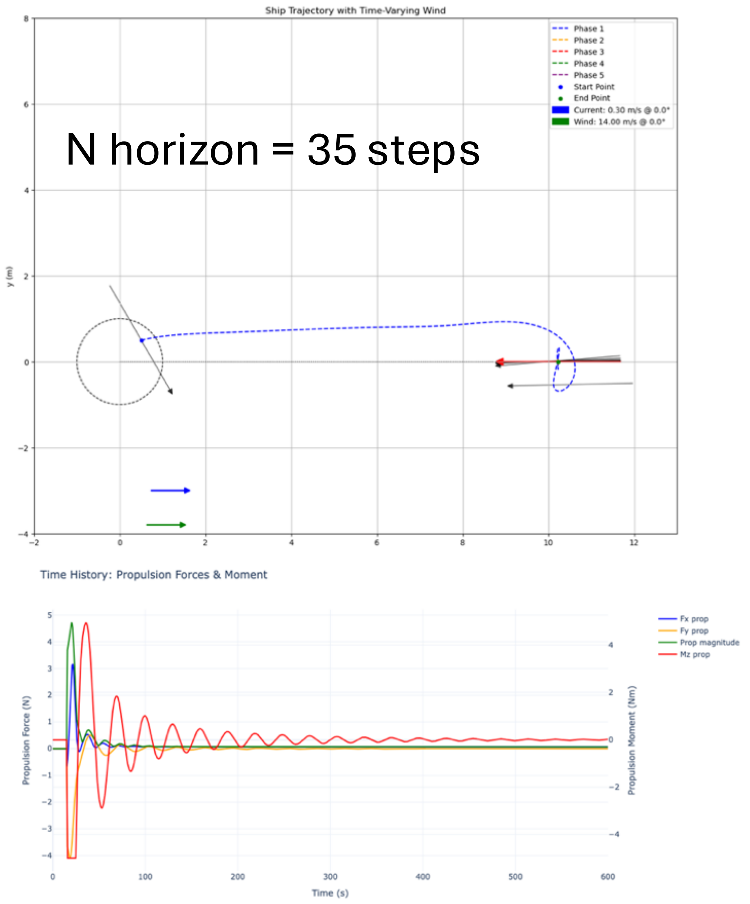

Scenarios tested:

Current (m/s)	Wind (m/s)
0	14
0.3	18
0.3	16
0.3	15
0.3	**14**
0.3	12
0.3	10
0.3	8

For combination of current and wind, 35 steps leads to complete stabilization

Trajectory (top) and propulsion (bottom) plots for MPC-controlled cases at wind speeds of 14 m/s, comparing prediction horizons of 30 steps (left) versus 35 steps (right) under a constant current of 0.3 m/s.

Control Results. MPC. b)

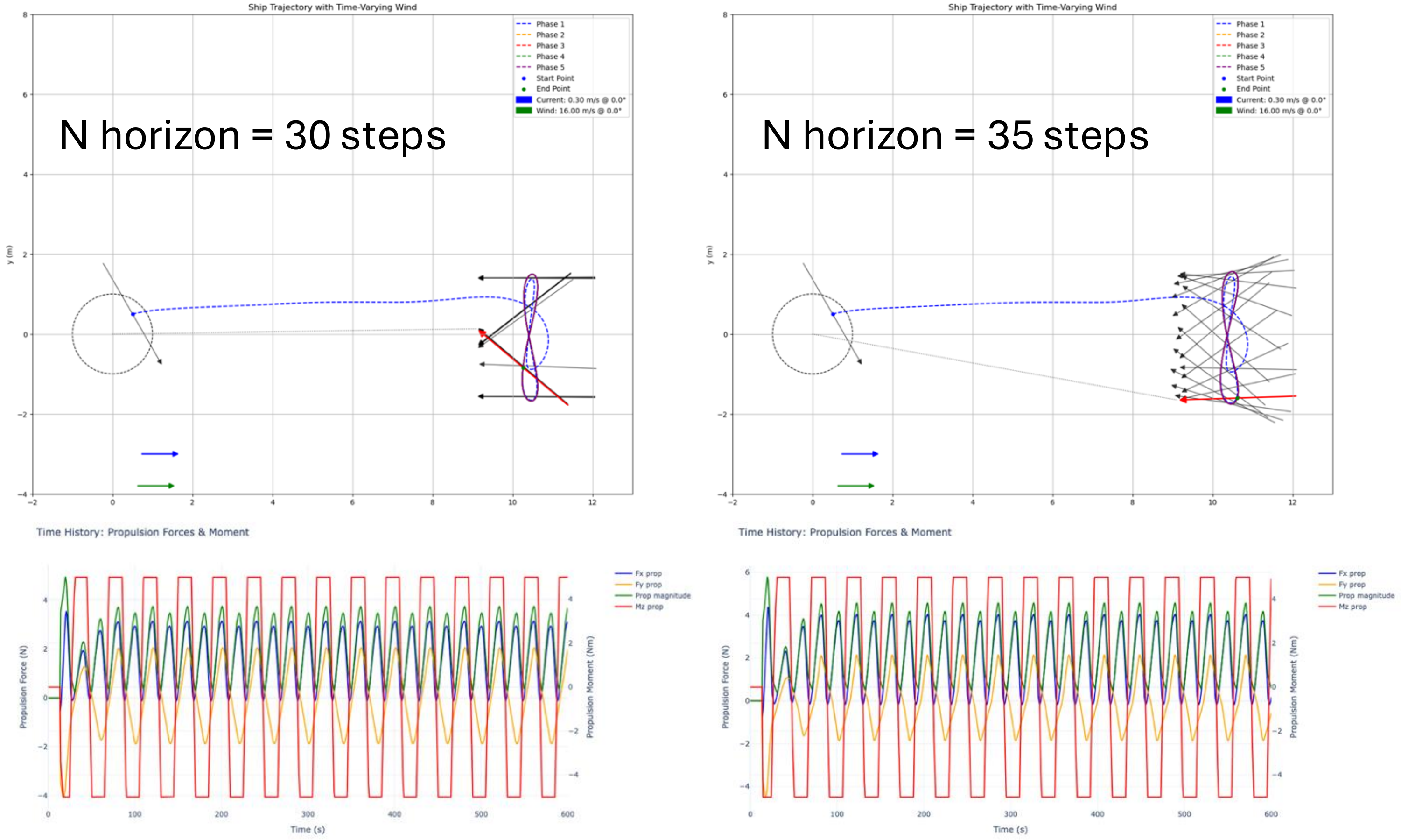

Trajectory (top) and propulsion (bottom) plots for MPC-controlled cases at wind speeds of 16 m/s, comparing prediction horizons of 30 steps (left) versus 35 steps (right) under a constant current of 0.3 m/s.

Scenarios tested:

Current (m/s)	Wind (m/s)
0	14
0.3	18
0.3	**16**
0.3	15
0.3	14
0.3	12
0.3	10
0.3	8

But for 16 m/s no enhancement.
Only slight difference in frequency can be noted..

Control Results. MPC. c) Dynamic gust

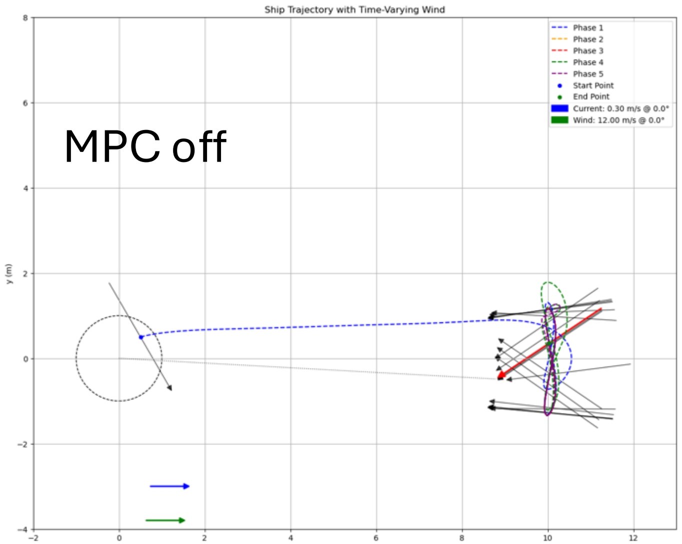

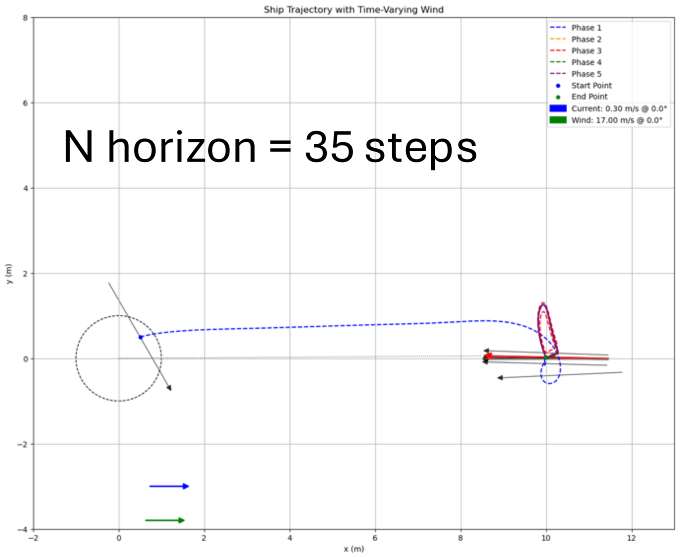

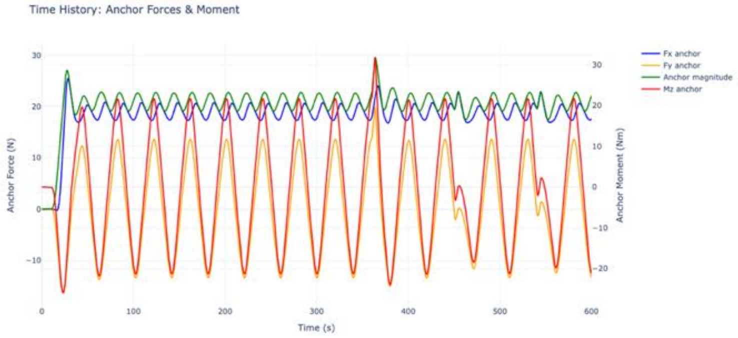

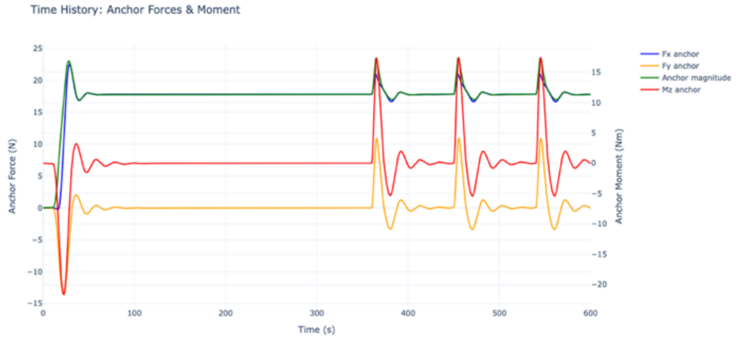

Gust scenario

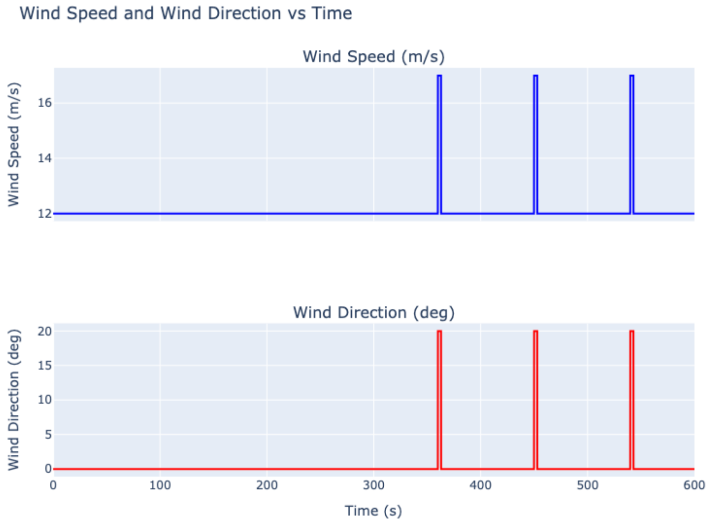

To test how controller returns system to a stable position after injected disturbance.

Trajectory and anchor force plots for dynamic gust scenarios (wind 12 m/s, current 0.3 m/s, gusts of +5 m/s from 20° every 90 seconds for 3 seconds) without (left) and with (right) MPC control.

Control Results. PD.

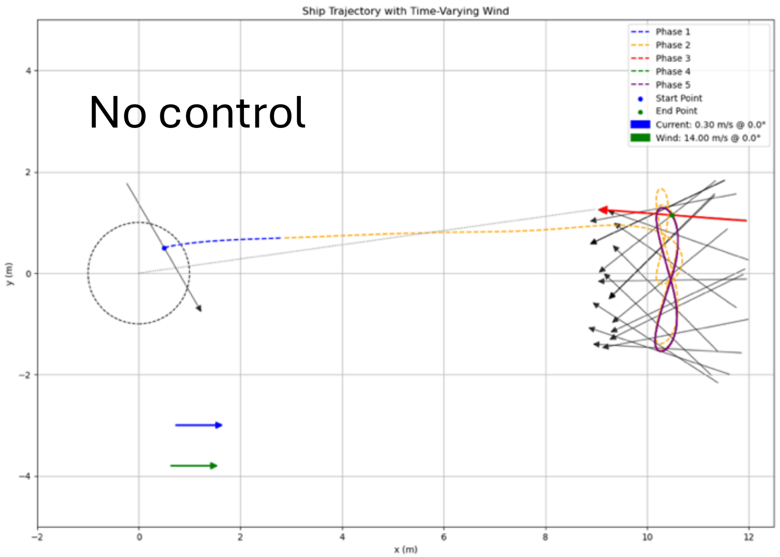

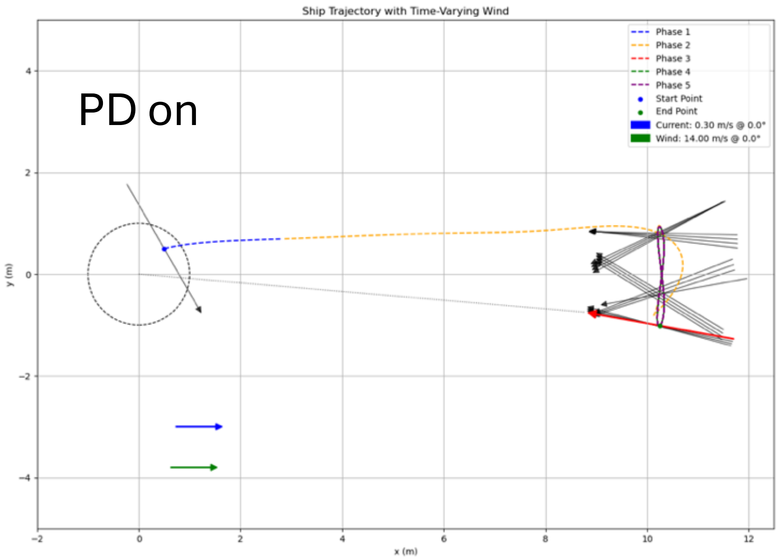

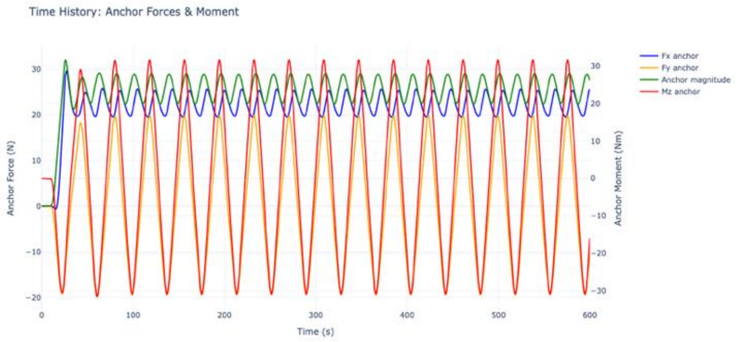

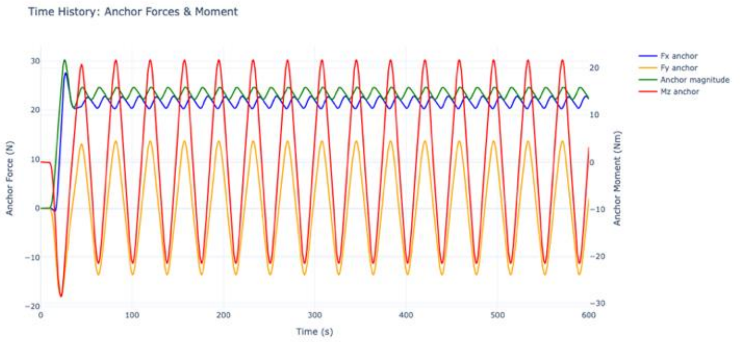

Trajectory and anchor force plots for wind speed=14 m/s and current=0.3 m/s without (left) and with (right) PD control.

Scenarios tested:

Current (m/s)	**Wind (m/s)**
0.3	18
0.3	16
0.3	15
0.3	**14**
0.3	12
0.3	10
0.3	8

PD gains after tuning:

Term	Sway	Yaw
Proportional	37.5	17.1
Derivative	83.8	−198.5

Control Results. Comparison.

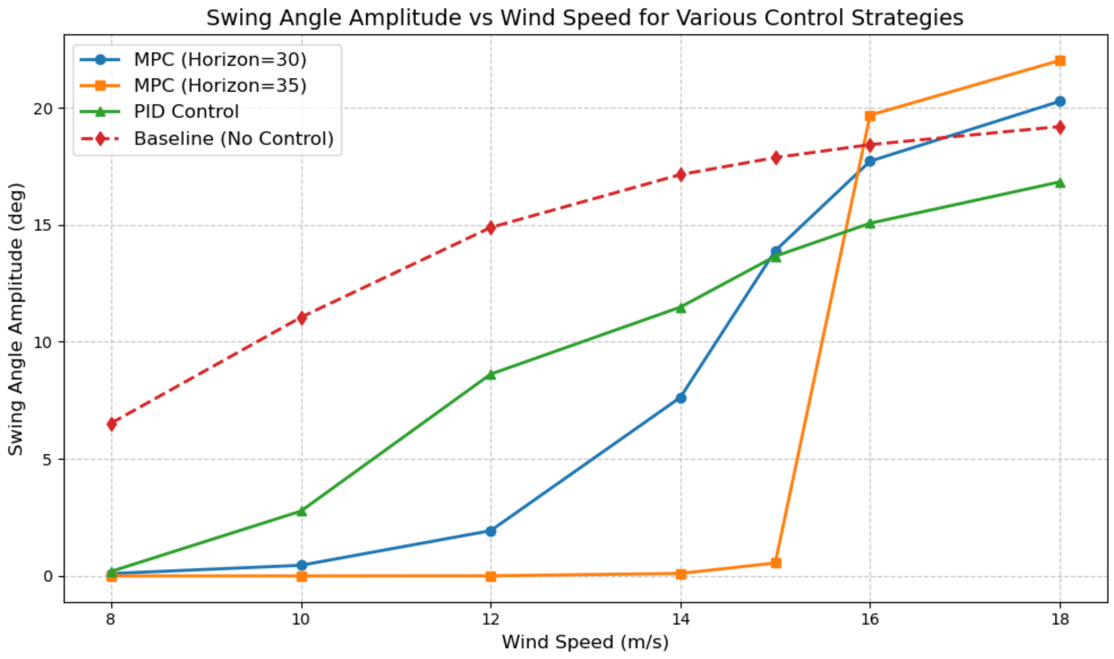

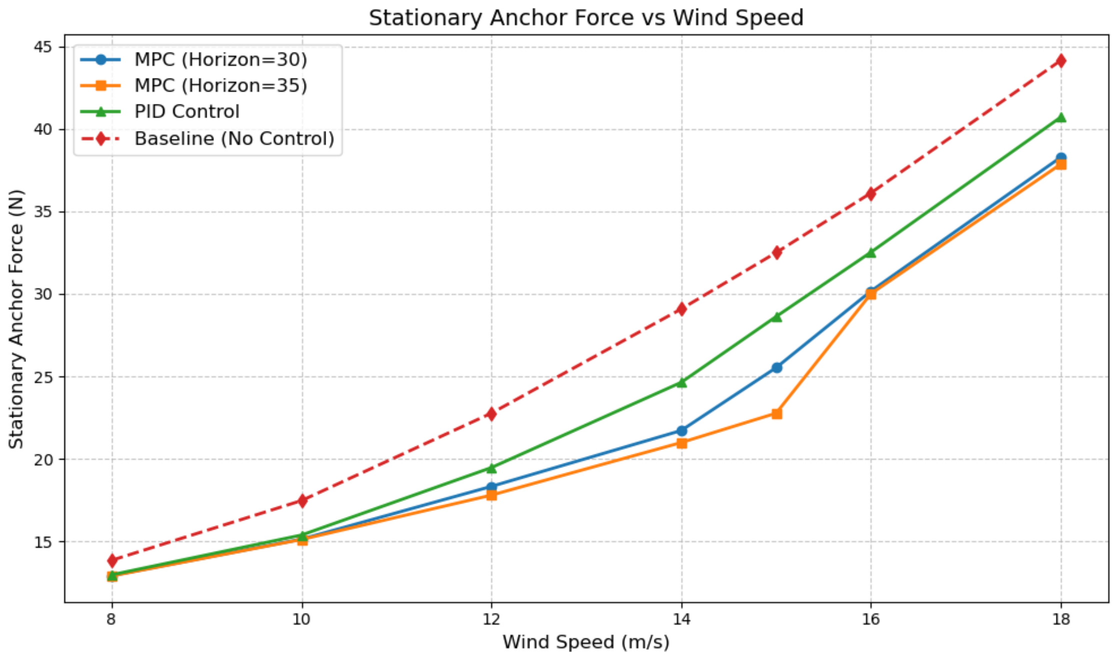

Control Results. Comparison.

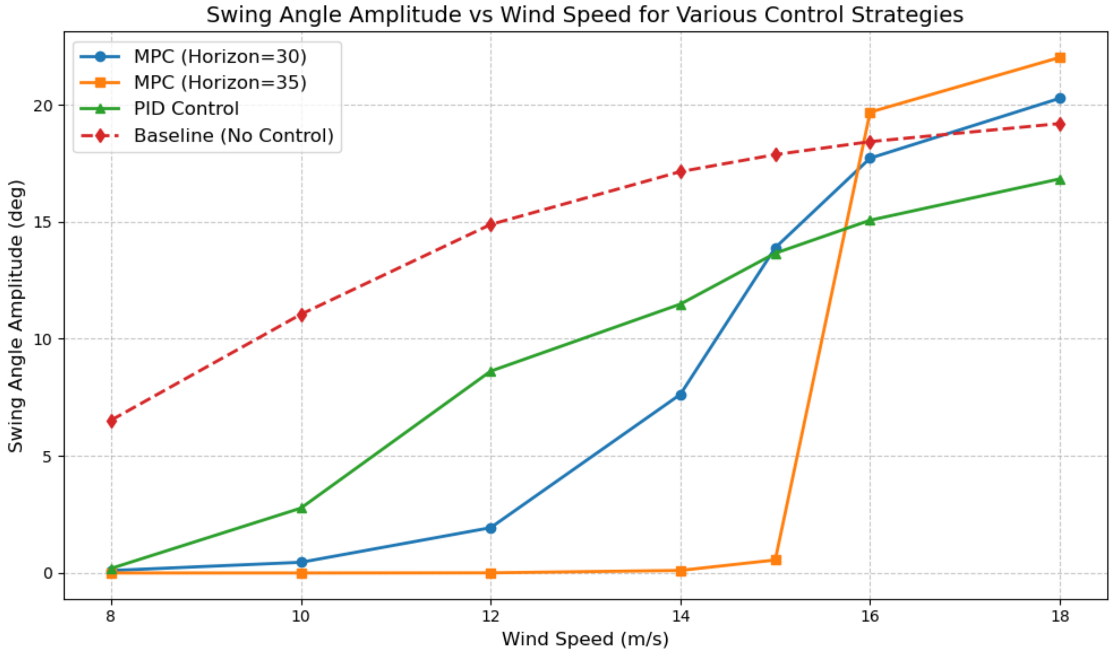

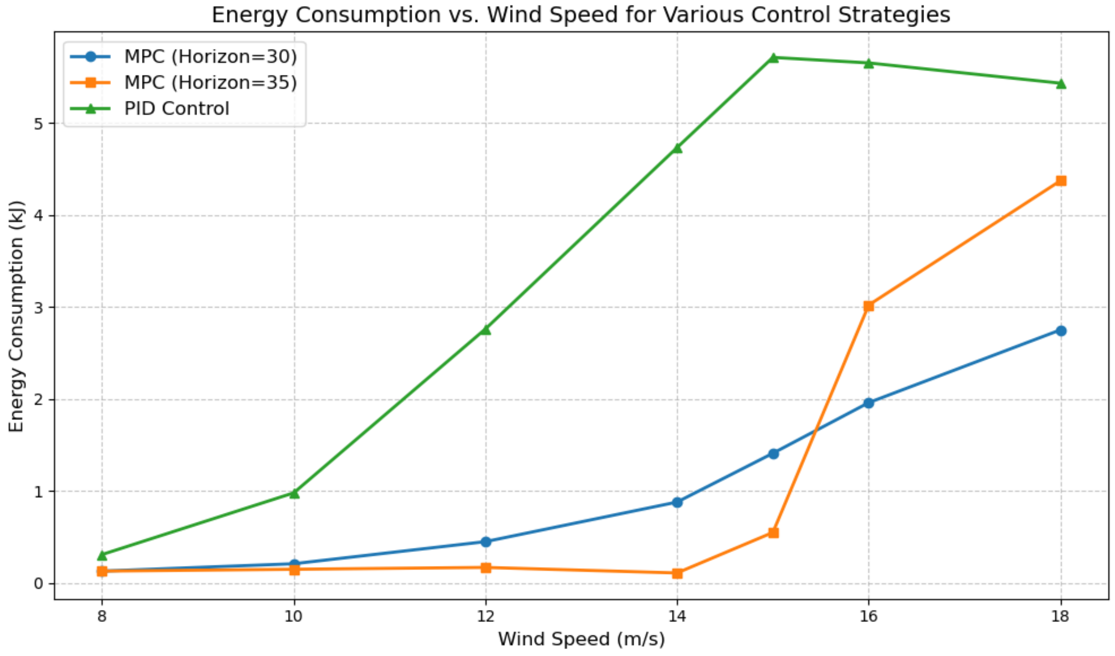

Conclusion

- 3-DoF dynamic model (Fossen's framework) captures vessel swing
- Model components:
    - 3 DoF
    - No Waves
    - No Thrust Allocation
    - Simplified anchor line dynamic (power-law)
    - Delft 372 – specific Hydrodynamic coefficients
- Wind & current interactions generate oscillatory patterns
- MPC: near-complete stabilization, low energy use in stable regime
- PD controller: moderate swing reduction, higher energy cost
- Findings inform autonomous maritime operations and anchoring strategy

Limitations and next steps

- 3-DoF Limitations: Misses heave, pitch, roll; 6-DoF needed
- Environmental Modeling: Idealized wind/current; omits wave effects
- Hydrodynamics: Coefficients require further calibration
- Anchoring/Thrusters: Simplified; lacks realistic elasticity and detailed propulsion dynamics
- Controller Robustness: Further Tuning; MPC sensitivity analysis; PD-gains optimization search
- Validation: Results based solely on simulations

References mentioned

- *Bahrin M, Othman F, Azli N, Talib M. 2016. Industry 4.0: a review on industrial automation and robotic. Jurnal Teknologi. 78.*
- *Hinz ER. 1986. The complete book of anchoring and mooring. Centreville (MD): Cornell Maritime Press.*
- *US Army Corps of Engineers. 2020. Design: moorings (UFC 4-159-03). Washington (DC): US Army Corps of Engineers.*
- *Flory J, Poranski P. 1977. The design of single point moorings. In: Proceedings of the 9th Annual Offshore Technology Conference; 1977 May 2–5; Houston, TX. Richardson (TX): Society of Petroleum Engineers.*
- *Okada T. 2018. Loss prevention bulletin Naiko class vol.4: ship maneuvering technical reference [Internet]. Tokyo (Japan): The Japan P&I Club; [accessed 2025 Feb 27]. Available from: https://www.piclub.or.jp/wp-content/uploads/2018/04/Loss-Prevention-Bulletin-Naiko-Class-Vol.4_Ship-Maneuvering-Technical-Reference.pdf*
- *Yoo SL, Onyango SO, Kim JS, Kim KI. 2024. Anchor dragging risk estimation strategy from supervised cost-sensitive learning. Journal of Marine Science and Engineering. 12:1817.*
- *Fossen TI. 2011. Handbook of marine craft hydrodynamics and motion control. Chichester (UK): Wiley.*
- *Yoshimura Y. 2005. Mathematical model for manoeuvring ship motion (MMG model).*
- *Mai TL, Nguyen TT, Jeon M, Yoon HK. 2020. Analysis on hydrodynamic force acting on a catamaran at low speed using RANS numerical method. Journal of Navigation and Port Research. 44(2):53–64.*
- *Van't Veer R. 1998. Experimental results of motions, hydrodynamic coefficients and wave loads on the 372 catamaran model. Technical Report No. 1129. Delft (Netherlands): Delft University of Technology*

Thank you!

Co-funded by the Erasmus+ Programme of the European Union

SUSTAINABLE SHIP AND SHIPPING 4.0

Erasmus Mundus Joint Master Degree

www.master-seas40.unina.it

Development of a Thruster-Assisted Single-Point Anchoring Model

Dmitrii Aparin

4 March 2025

Supervisor: Prof. Smilko Rudan

University of Zagreb

Università degli studi di Napoli Federico II

Universidade da Coruna

Academic Year 2024/2025

Technische Universität Hamburg